Öppen

Report

Document ID	Version	Status	Reg no	Page
1417006	1.0	Godkänt		1 (47)
Author Auqué, Luis F. Acero, Patricia Gimeno, María J. Gómez, Javier Puigdomenech, Ignasi			Date 2013-11-12	
Reviewed by			Reviewed date	
Approved by Allan Hedin			Approved date 2013-12-19	

Effects of weathering of silicate minerals and cation-exchange on the geochemical safety indicators during the hydrogeochemical evolution at Forsmark

Svensk Kärnbränslehantering AB
Swedish Nuclear Fuel and Waste Management Co
PO Box 250, SE-101 24 Stockholm
Visiting address Blekholmstorget 30
Phone +46-8-459 84 00 Fax +46-8-579 386 10
www.skb.se
556175-2014 Seat Stockholm

Table of Contents

1 Introduction

In the framework of the SR-Site assessment (SKB 2011) a reduced set of mineral reactions to be in equilibrium with the groundwaters (calcite, quartz, hydroxyapatite and either Fe-oxyhydroxide or "amorphous" FeS) was chosen in the mixing and reaction simulations (Gimeno et al. 2010, Salas et al. 2010). They were selected either because they have fast precipitation/dissolution kinetics compared with the simulated time intervals (calcite) or because they are in apparent equilibrium in the present groundwaters (quartz; Gimeno et al. 2008, 2009, 2010). However, they represent only a limited subset of the minerals present in the fractures. Other minerals like chlorite, illite or K-feldspar, frequently found in the fracture fillings, could also participate in dissolution or precipitation reactions, as indicated by Salas et al. (2010, section 9.5.2.) and Gimeno et al. (2010, section 6.1.2).

The specific case of aluminosilicates is commented in the SR-Site reports indicating the arguments why they were not included in the set of equilibrium minerals. The first reason was the difficulty in justifying which thermodynamic data to use, due to their considerable uncertainties (as they depend on the particular mineral composition, crystallinity, degree of order/disorder, *etc*). The second reason is that previous scoping calculations performed for SR-Can by Auqué et al. (2006) showed that including chlorite and illite equilibria in the calculations had insignificant effects on the concentrations of magnesium and potassium; so these minerals did not contribute with additional information to the model results.

Neither were cation exchange processes, despite their potential importance, included in the final Forsmark report for SR-Site (Salas et al. 2010) for several reasons, mainly that: a) the calculation methodology was under development and testing at that time; and b) the available data on the cation exchange capacity (CEC) values for fracture filling minerals were unavailable or very scarce and uncertain. Nevertheless some sensitivity analysis on the influence of cation exchange processes was presented by Gimeno et al. (2010) in the calculations for Laxemar.

In this context, SSM has asked SKB to provide additional information about the effects of the excluded reactions (aluminosilicate weathering and ion-exchange) on the geochemical safety indicators used in SR-Site.

The intention of this document is to show:

- That adding aluminosilicate weathering reactions in the groundwater geochemical modelling of Forsmark can have a large effect on the calculated concentrations of "minor" components such potassium, and on pH. Thus, it is questionable if accurate conclusions may be reached about such groundwater characteristics based exclusively on modelling. Modelling may still provide sufficient bounds to ensure that relevant safety functions indicator criteria would not be breached.
- On the contrary, adding aluminosilicate reactions to the groundwater modelling has a negligible effect on "major", *i.e.* soluble, components such as calcium, sodium, chloride, *etc*.
- Data from a few granitic rock sites corroborates the last point: weathering reactions alone have practically no influence on the salinity and "major" components of groundwaters, because many sites exist where deep groundwaters have long average residence times, with enough time for aluminosilicate weathering to take place, but with salinities not much higher than those of the recharging waters. This depends naturally on the geological and hydrogeological conditions and, for example, there are other sites in granitic rocks, with equally "old" or even younger groundwaters, that have groundwaters with high salinity, which has other origins than aluminosilicate weathering.
- Cation-exchange processes may alter the ratio between cations in the groundwaters, for example sodium/calcium, but the total concentration of cationic charges remains unchanged, and therefore they have no effect on the safety function indicator R1c of SR-Site ($\sum q[M^{q+}] > 4$ mM charge equiv.).
- The estimated values for the safety function indicators R1e (pH) and R1d (potassium) do not violate the safety criteria by the inclusion of ion-exchange equilibrium reactions.

It may be noted here that for a case with an extended temperate period at Forsmark it is to be expected that groundwaters will become predominantly of meteoric origin, at least in the upper volumes of the rock, and the groundwaters would then become more and more controlled by water-rock interaction processes, enhancing the importance of mineral dissolution/precipitation and cation exchange processes when evaluating the groundwater evolution.

2 Weathering of aluminosilicates

The uncertainties and conceptual problems related to the inclusion of aluminosilicate phases, and especially clay minerals, in modelling low temperature systems (even in the "simple" thermodynamic equilibrium approach used in this work) are widely recognised (e.g. Wilson et al. 2006) and still represent an unsolved problem in geochemical modelling. Dealing with these mineral phases needs, at the very least, some type of sensitivity analysis more or less complex depending on the number and specific type of the aluminosilicate minerals of interest, the key parameters in the simulations, *etc*. The calculations and results presented in this document are focussed on the geochemical safety indicators used in SR-Site, as requested by the SSM. Therefore, mixing and reaction simulations using some of the selected hydrochemical data in the calculations performed by Salas et al. (2010) have been repeated here, prescribing additional aluminosilicate minerals at equilibrium. In the present calculations a limited sensitivity analysis has been performed with respect to 1) the number and/or type of aluminosilicates included in the calculations and 2) their equilibrium constants (solubility products).

Effects of aluminosilicate reactions on the safety function indicators, other than redox related (the effects of iron silicates on the redox evolution were considered in the calculations on oxygen inflow performed by Sidborn et al. (2010)) are evaluated here. The calculated pH (safety function indicator R1e, pH<11), the value of $\Sigma q[M^{q+}]$ (cation safety function indicator R1c, $\Sigma q[M^{q+}] > 4$ mM) and the dissolved potassium concentration (safety function indicator R1d; SKB 2011) are potentially most directly affected by the weathering of aluminosilicates.

The aluminosilicate minerals considered in the calculations have been selected from those present as fracture fillings in conductive fractures at Forsmark, as explained in the next section.

2.1 Aluminosilicates in the fracture fillings at Forsmark

Different aluminosilicates have been identified in the fracture fillings at Forsmark. Chlorite (usually associated with corrensite) and calcite are, by far, the most common fracture minerals. But, also, feldspars, other clay minerals and zeolites have been found in different proportions. Overall, the relative abundance of the different mineral phases found in all type of fractures (open and sealed) is as follows (Löfgren and Sidborn 2010, Sandström et al. 2008): calcite and chlorite/corrensite >> laumontite > quartz, adularia, albite, clay minerals > prehnite, epidote > haematite and pyrite. Some other minerals may be more common in specific intervals or at shallow depths (e.g. asphaltite, analcime and goethite), and others (e.g. apophyllite, fluorite, galena) have only been found as minor occurrences.

The identification of clay minerals (other than chlorite) and their relative proportions were based on the available XRD data, mostly for hydraulically conductive fractures (Sandström et al. 2008). From this information, corrensite (a chlorite-like mixed-layer clay with layers of chlorite and smectite/vermiculite, usually with a ratio of 1:1) is the dominant clay mineral followed by illite and mixed layer clays (e.g. illite/smectite). Non-mixed smectite, vermiculite and kaolinite have also been identified, but only in a few samples (Figure 2-1).

The aluminosilicates are widely distributed with depth and no significant trends can be identified. In the case of the clay minerals (Figure 2-2) kaolinite was identified only in two observations at shallow depths and vermiculite was identified only in one sample at around 300 m depth. Saponite (a variety of swelling smectite) was also identified but only in two samples, at around 400 and 900 m depth. No samples with corrensite were identified in the upper 75 m of the bedrock (Figure 2-2) although this observation can be related to sampling problems (Sandström et al. 2008).

Some differences in the distribution have been found depending on the type of fracture and on the fracture domain. Clay minerals (other than chlorite) are not evenly distributed in the open fractures: they are found more abundantly in the upper 200 m of the bedrock and, especially, in fractures with an aperture larger than 1 mm (Drake et al. 2006); and they occur most abundantly in open fractures from the FFM02 domain (Löfgren and Sidborn 2010, Sandström et al. 2008).

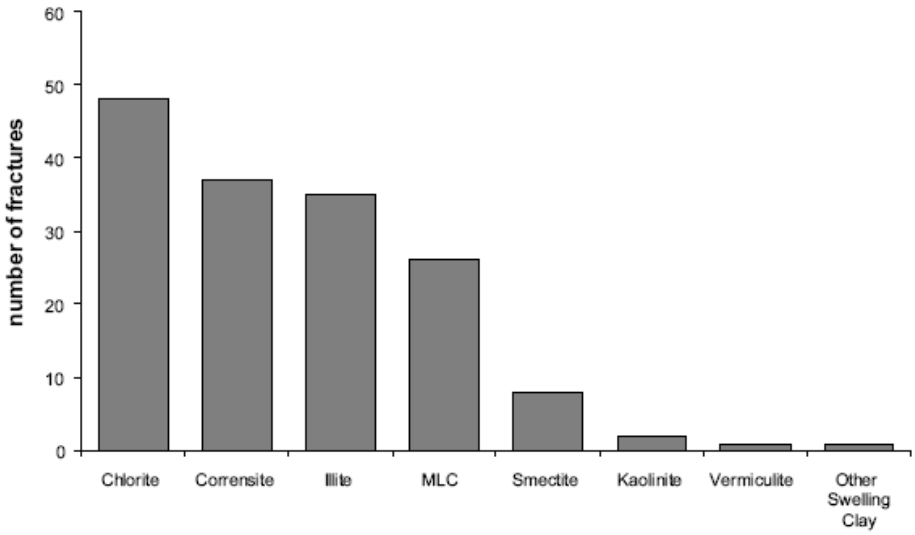

Figure 2-1. *Histogram showing the number of fractures (mostly hydraulically conductive fractures), where clay minerals and chlorite have been identified by XRD-analysis of bulk fracture filling material in the fine fraction (< 10 µm). MLC = mixed layer clay. From Sandström et al. (2008).*

With respect to the other aluminosilicates, laumontite (a zeolite) is in general less common in open fractures in the upper 100 metres. Furthermore, when only the few hydraulically conductive fractures (showing PLF flow log anomalies) are considered, the most striking feature is the small number of fractures containing laumontite. This may be due to breakdown of this easily decomposed mineral (Sandström et al. 2008).

The study of feldspars distribution (albite and adularia, a hydrothermal K-feldspar) is not so detailed but, apparently, the presence of these minerals has been indicated in sealed and conductive fractures in the whole range of examined depths (Sandström et al. 2008).

From this brief overview, and based on their abundance and/or presence in the hydraulically conductive fractures, some aluminosilicates have been chosen as the most suitable for the simulations: chlorite, illite, smectites and feldspars.

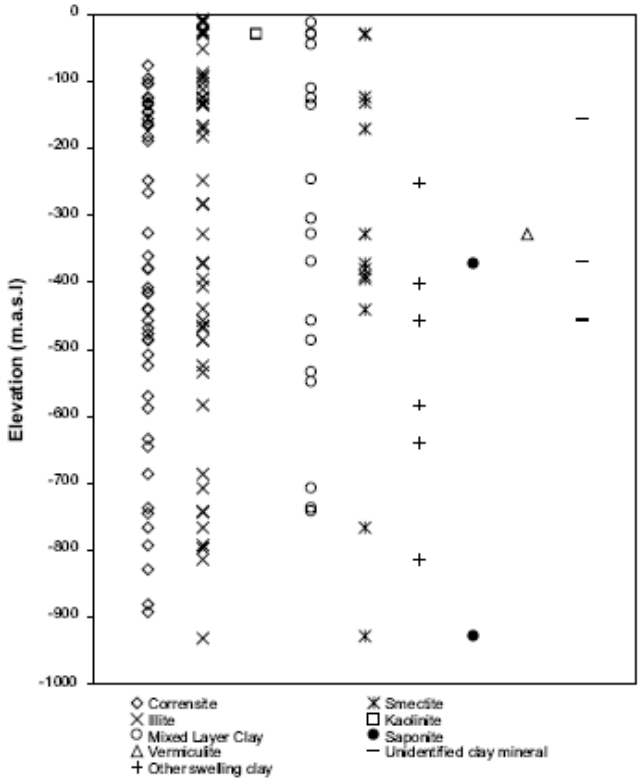

Figure 2-2 *Presence of different clay minerals identified by XRD with depth. From Sandström et al. (2008).*

2.2 Mixing and reaction simulations with aluminosilicates

The reaction kinetics of the selected aluminosilicate phases (chlorite, illite, smectites and feldspars) is slow, particularly in the case of dissolution of pure Na- and K-feldspar (Gérard et al. 1998, Lasaga et al. 1994) which contributes slowly to the water composition at pH buffered by the presence of calcite in granitic systems (Bucher et al. 2009). The dissolution rate of smectites (montmorillonites) in granitic groundwaters under neutral-basic pH is slower than those of many common silicates (Cama et al. 2000, Huertas et al. 2001) and in the same range as that of illite (Köhler et al. 2003). In fact, dissolution processes of smectite (montmorillonite) or illitization processes in the buffer have usually been neglected in the calculations for the evolution of the near-field in the safety assessment calculations in the long term (60,000-100,000 years; *e.g.* Arcos et al. 2006, Sena et al. 2010).

Kinetic constraints are important when dealing with this type of mineral phases and they are partly responsible for the clay mineral assemblages observed in natural systems (*e.g.* Wilson et al. 2006). Thus, a kinetic approach would be*, a priori*, more appropriate in modelling a groundwater system with such low reaction rates for the involved minerals (*e.g.* Bath 2011).

However, in the framework of site characterisation programmes, thermodynamic equilibrium conditions with respect to aluminosilicate phases have been considered when modelling long residence time groundwaters (*e.g.* 20,000 years) in low temperature granitic and argillaceous

systems (*e.g.* Beaucaire et al. 2008, Gaucher et al. 2009, Grimaud et al. 1990, Pearson et al. 2011, Tournassat et al. 2011, Trotignon et al. 1999).

In this work some aluminosilicate phases have been forced to reach equilibrium in mixing and reaction calculations. This approach, although perhaps unrealistic, allows evaluating the effect of the strongest possible influence of aluminosilicate reactions on groundwater hydrochemistry. As an additional advantage, this approach eliminates the large uncertainties associated with the reaction kinetics of the considered mineral phases (lack of experimental or field rates, unknown reactive surfaces and relative abundances, *etc*). However, the uncertainties in the thermodynamic data for this type of mineral phases remains (*e.g*. Beaucaire et al. 2008, Gaucher et al. 2009, Trotignon et al. 1999, Wersin et al. 2011).

A systematic review on the available thermodynamic data (poorly constrained in the case of clay minerals) for these mineral phases and their related uncertainties and a full sensitivity analysis on the propagation of these uncertainties in the results is not carried out in this work. Instead the more pragmatic approach presented in Gaucher et al. (2009), using two sets of thermodynamic data different enough, has been used. This approach has been applied on a reduced number of waters from the original set of hydrochemical data used in the calculations performed by Salas et al. (2010). Moreover, given the large uncertainty about the possible influence of different aluminosilicates, different sets of equilibrated mineral phases have been considered as test cases.

The selection of the hydrochemical and thermodynamic data for the present assessment and the defined test cases are explained in the next sections.

2.2.1 Selection of representative samples for the geochemical modelling tests

The influence of aluminosilicate reactions will be negligible during the first thousands of years after the closure of the repository, since the reaction kinetics of these phases is typically quite slow. It is expected that the strongest impact of these processes in the repository hydrochemistry, if any, would occur after this initial period. For this reason, the calculations presented here have been done using the calculated mixing proportions of the samples at 9000 AD (Salas et al. 2010) as the starting point. The original set of data had compositions for more than 65,000 grid locations in the repository vicinity. In order to reduce the number of data without losing the hydrochemical representativity, a screening of the available compositions has been carried out and 45 calculated groundwater compositions for 9000 AD have been selected (Table *2-1*). These hydrochemical data represent six sets of different and extreme groundwater compositions, according to their corresponding mixing proportions of the Deep Saline, Glacial, Littorina, Old Meteoric and Altered Meteoric end members. Groups of waters representative of the largest mixing proportions of each of those end members have been selected and, within these groups, the variable influence of the input of altered meteoric waters has also been used as a sub-criterion. The reason for this sub-criterion is the key influence that the input of the meteoric waters will have on the site hydrochemistry in the medium-long term due to the expected hydrogeological conditions and processes during the extended temperate period (Salas et al. 2010).

Table 2-1. Set of selected water compositions chosen to represent the variable hydrochemistry expectable at repository depth in the present assessment. The proportion of Deep Saline, Glacial, Littorina, Old Meteoric and Altered Meteoric end members corresponding to each of them is also detailed, together with the screening criteria applied for their selection (see text for details).

% Mixing end members					Reason for inclusion in the calculations
DS	Litt	AM	Gl	OM	
0.004	0.076	99.885	0.017	0.017	largest % AM (almost pure)
0.004	0.071	99.894	0.016	0.016	largest % AM (almost pure)
0.004	0.072	99.891	0.017	0.018	largest % AM (almost pure)
0.004	0.071	99.892	0.017	0.017	largest % AM (almost pure)
0.003	0.065	99.901	0.016	0.016	largest % AM (almost pure)
0.004	0.073	99.888	0.018	0.018	largest % AM (almost pure)
0.004	0.038	99.933	0.006	0.019	largest % AM (almost pure)
0.004	0.072	99.889	0.018	0.018	largest % AM (almost pure)
0.003	0.068	99.895	0.017	0.017	largest % AM (almost pure)
0.003	0.064	99.901	0.016	0.016	largest % AM (almost pure)
0.000	0.028	99.953	0.003	0.016	largest % AM (almost pure)
0.004	0.070	99.891	0.018	0.018	largest % AM (almost pure)
0.004	0.067	99.894	0.017	0.018	largest % AM (almost pure)
0.004	0.041	99.932	0.006	0.018	largest % AM (almost pure)
0.000	0.030	99.954	0.002	0.014	largest % AM (almost pure)
16.551	14.201	4.066	21.711	43.472	minimum AM among samples with largest % DS
16.840	11.370	3.618	23.100	45.071	minimum AM among samples with largest % DS
16.480	11.860	13.570	17.570	40.520	minimum AM among samples with largest % DS
16.450	10.730	14.030	17.710	41.080	minimum AM among samples with largest % DS
16.649	5.884	4.240	24.369	48.858	minimum AM among samples with largest % DS
16.450	6.947	14.700	21.481	40.421	minimum AM among samples with largest % DS
16.831	6.508	4.107	26.531	46.022	minimum AM among samples with largest % DS
16.521	7.826	18.781	19.101	37.771	minimum AM among samples with largest % DS
16.529	7.676	15.339	20.709	39.747	minimum AM among samples with largest % DS
16.640	6.579	3.959	26.751	46.071	minimum AM among samples with largest % DS
2.197	57.961	7.672	21.060	11.110	minimum AM among samples with largest % Litt
1.007	58.181	20.650	13.900	6.261	minimum AM among samples with largest % Litt
1.396	56.481	19.990	14.850	7.283	minimum AM among samples with largest % Litt
2.463	58.452	6.034	21.601	11.450	minimum AM among samples with largest % Litt
0.940	56.273	23.491	13.361	5.935	minimum AM among samples with largest % Litt
2.900	56.529	5.131	22.850	12.590	minimum AM among samples with largest % Litt
2.599	58.079	8.162	19.510	11.650	minimum AM among samples with largest % Litt
2.623	58.272	6.533	21.681	10.890	minimum AM among samples with largest % Litt
1.050	56.725	20.002	15.021	7.203	minimum AM among samples with largest % Litt
14.050	3.274	0.153	45.421	37.101	maximum AM among samples with largest % Gl
14.040	3.248	0.151	45.441	37.120	maximum AM among samples with largest % Gl
13.971	3.369	0.155	45.603	36.902	maximum AM among samples with largest % Gl
13.870	3.732	0.210	45.389	36.799	maximum AM among samples with largest % Gl
13.911	3.525	0.190	45.492	36.882	maximum AM among samples with largest % Gl
13.820	3.806	0.226	45.429	36.719	maximum AM among samples with largest % Gl
1.041	56.621	21.060	14.530	6.747	maximum AM among samples with largest % Litt
14.300	2.942	0.150	45.339	37.269	maximum AM among samples with largest % Gl
14.330	2.842	0.140	45.399	37.289	maximum AM among samples with largest % Gl
14.210	3.140	0.173	45.378	37.099	maximum AM among samples with largest % Gl
14.159	3.245	0.211	45.317	37.068	maximum AM among samples with largest % Gl

DS: Deep Saline; Litt: Littorina; AM: Altered Meteoric; Gl: Glacial; OM: Old Meteoric

2.2.2 Thermodynamic data

As stated above, several mineral phases have been chosen based on their possible presence in the repository surroundings and on their representativity of different types of phases which could affect the site hydrochemistry. These phases are: chlorite, K-feldspar, albite, illite and smectite group minerals. For some of these minerals, different varieties have also been included in the calculations whenever their thermodynamic data are available in the used databases.

For the selection of the appropriate thermodynamic data for the selected minerals, different thermodynamic databases have been considered:

- The thermodynamic database used in SR-Site (SKBdoc id 1261302, vers.3.0, referred in this document as "TDB_SKB-2009_Amphos21").
- The WATEQ4F database distributed with PhreeqC.
- The LLNL (Lawrence Livermore National Laboratory) database distributed with PhreeqC.
- THERMODDEM database (from BRGM, France, see below).
- SIT (Specific Ion Interaction Theory) database distributed with PhreeqC.

During the examination of these databases, one of the main problems was the lack of consistence and coincidence among the data contained in each of them. The number of phases and mineral varieties included in each database is notably different and, moreover, the thermodynamic data associated with apparently identical phases are frequently also variable. For instance, in the case of the database used for the SR-Site calculations (Gimeno et al. 2010, Salas et al. 2010), none of the target minerals is included.

From the rest of the examined databases, LLNL, THERMODDEM and SIT contain an important number of aluminosilicates and, specially, clay minerals. The LLNL database distributed with PHREEQC (and also with the EQ3/6 or with the Geochemist´s Workbench codes, as "thermo.com.V8.R6.230" database) contains the largest set of aluminosilicate phases, including the widest variety of clay minerals and it is widely used in the geochemical modelling of aluminosilicate reactions (Aradóttir et al. 2012, Bucher et al. 2009, Klein et al. 2013, Stumpf et al. 2012 among others) even in the context of nuclear waste repository performance assessment, e.g. (Bath 2011).

The SIT database corresponds to the ANDRA database ThermoChimie v.8 SIT database (released for the first time as "sit.dat" database with PHREEQC v.17) developed by Amphos 21, BRGM and HydrAsa.

The THERMODDEM database developed by BRGM, ANDRA and ADEME (free available on Nov.2013 at http://thermoddem.brgm.fr) is very similar as most of the sources for thermodynamic data are common in both databases. For example, both include recent experimental data (Gailhanou et al. 2007, 2009, 2012) and theoretical estimations of the thermodynamic properties of clay minerals (Vieillard 2000, 2002).

The WATEQ4F database (Ball and Nordstrom 1991) distributed with PhreeqC also includes different aluminosilicate phases of interest in this assessment. This database was used in the scoping calculations with aluminosilicate phases performed in (Auqué et al. 2006) in the framework of SR-Can. The results indicated that considering chlorite and illite from that database in the mixing and reaction calculations had insignificant effects on the concentrations of magnesium and potassium, and therefore this database was excluded in the present assessment.

For these reasons, we decided to carry out the geochemical calculations using the database with the largest number of phases, the LLNL database, and to perform a sensitivity analysis with the THERMODDEM database. The calculations have been performed with the code PHREEQC version 2.18 (Parkhurst and Appelo 1999).

2.2.3 Test cases

Given the large uncertainty about the possible influence of different aluminosilicates, five different cases have been tested in the calculations, each of them including a different set of equilibrated mineral phases (detailed in Table *2-2*). The results obtained by each of these cases have been compared with the ones obtained without imposing equilibrium with aluminosilicates (Base Case).

Table 2-2. Summary of the conditions tested in the geochemical calculations aimed at evaluating the potential effect of aluminosilicate dissolution on the long term hydrochemistry of the repository surroundings.

Case name	Calcite	Quartz	Apatite	Fe-oxyhydroxide	K-feldspar	Albite	Kaolinite	Illite	Chlorite	Smectite	Montmorillonite
Base case	x	x	x	x							
Test case 1	x	x	x	x	x	x					
Test case 2	x	x	x	x				x	x		
Test case 3	x	x	x	x				x		x	
Test case 4	x	x	x	x				x			x
Test case 5	x	x	x	x	x	x	x				

In Test Case 1, equilibrium with respect to albite and K-feldspar is imposed. This case could be considered as representative of a very long residence time for the groundwaters after mixing.

Test Cases 2 to 5 represent the reaction of the main mineral aluminosilicate groups described in the fracture filling from the bedrock at Forsmark (see section above "Aluminosilicates in the fracture fillings at Forsmark"). These phases are illite, chlorite and smectite-group minerals. In case 5 kaolinite was added: although it is not a common fracture filling mineral (section 2.1), it represents a common aluminosilicate produced in weathering reactions, and this case is similar to one of the cases included in the calculations reported in SKBdoc id 1416908 (Joyce et al. 2013). For all these cases, two different varieties of each chlorite and smectite present in the LLNL database have been checked. Moreover, calculations with four varieties of montmorillonite-type smectites have also been tested to represent smectite-group aluminosilicates.

In addition to the aluminosilicate minerals, equilibrium with respect to calcite, quartz, hydroxyapatite and Fe-oxyhydroxide (using the thermodynamic data proposed by Grenthe et al. 1992) has been imposed in all the geochemical calculations, consistently with the approach and

assumptions already adopted for the calculations at Forsmark (Salas et al. 2010). This mineral equilibrium set (calcite, quartz, hydroxyapatite and Fe-oxyhydroxide) has been considered here as the reference to compare the results obtained in the different Test Cases.

As an additional check, the same cases were also tested with the THERMODDEM database, which also features a reasonably large set of aluminosilicate data. Since the correspondence between the aluminosilicate varieties and thermodynamic data in the THERMODDEM and LLNL databases are not fully consistent, the most similar mineral formulae in THERMODDEM were chosen for this testing.

2.2.4 Calculation results

Results of the performed calculations indicate that the incorporation of aluminosilicate phases (as additional equilibrium conditions) in the mixing and reaction simulations promotes changes more or less important in the individual cation contents or in the pH values with respect to those of the Base Case.

Dissolved sodium, calcium and magnesium usually show minor variations with respect to the Base Case. Some changes can be observed, also depending on the selected chlorite, smectite or montmorillonite in Tests Cases 2, 3 and 4, but they are not significant in terms of the present discussion. For instance, variations in dissolved sodium (Figure 2-3) are undistinguishable at the scale of the graphs.

However, ***potassium results*** show a wider variability, see Figure 2-4 which shows that much lower concentrations are obtained in the Test Case 1 and 5 (always below 4 mg/L; Figure 2-4A) where K-feldspar and albite equilibria is imposed (Table *2-2*) although dissolved sodium contents are barely affected (Figure 2-3A). In Test Cases 2 and 3, aluminosilicate re-equilibrium promotes some minor changes in the potassium contents with respect to those obtained in the Base Case (Figure 2-4 B,C) and dissolved potassium is controlled mainly by mixing (in the Base Case potassium is considered a conservative element as it also was considered in Salas et al. (2010).

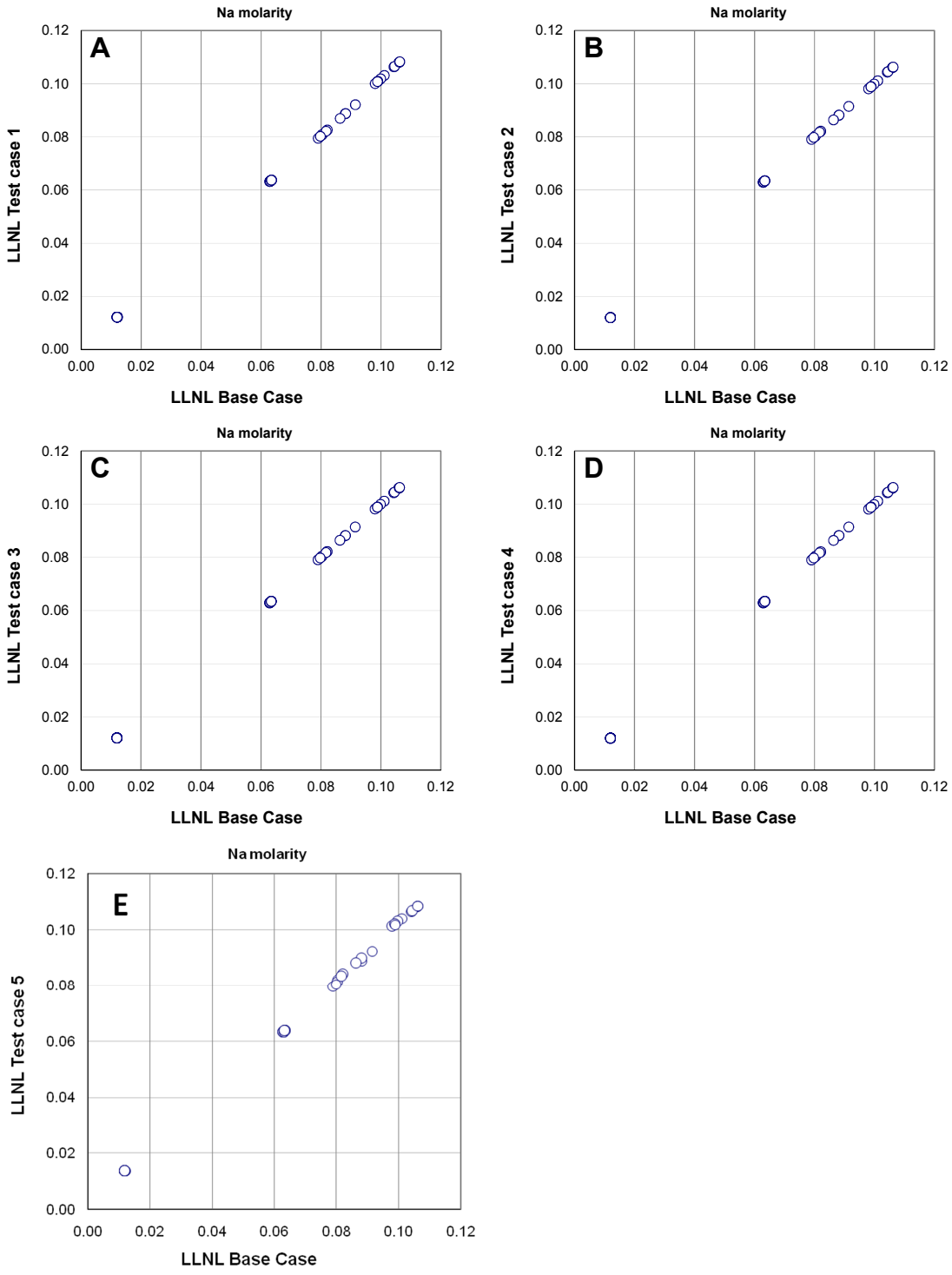

Figure 2-3. *Comparison between the obtained sodium concentrations (in mol/L) in the simulations carried out for the Test Cases 1 to 5 (panels A to D, respectively; see conditions in Table 2-2) and in the simulations done for the Base Case (without aluminosilicate reactions) in the earlier SR-Site calculations performed by Salas et al. (2010).*

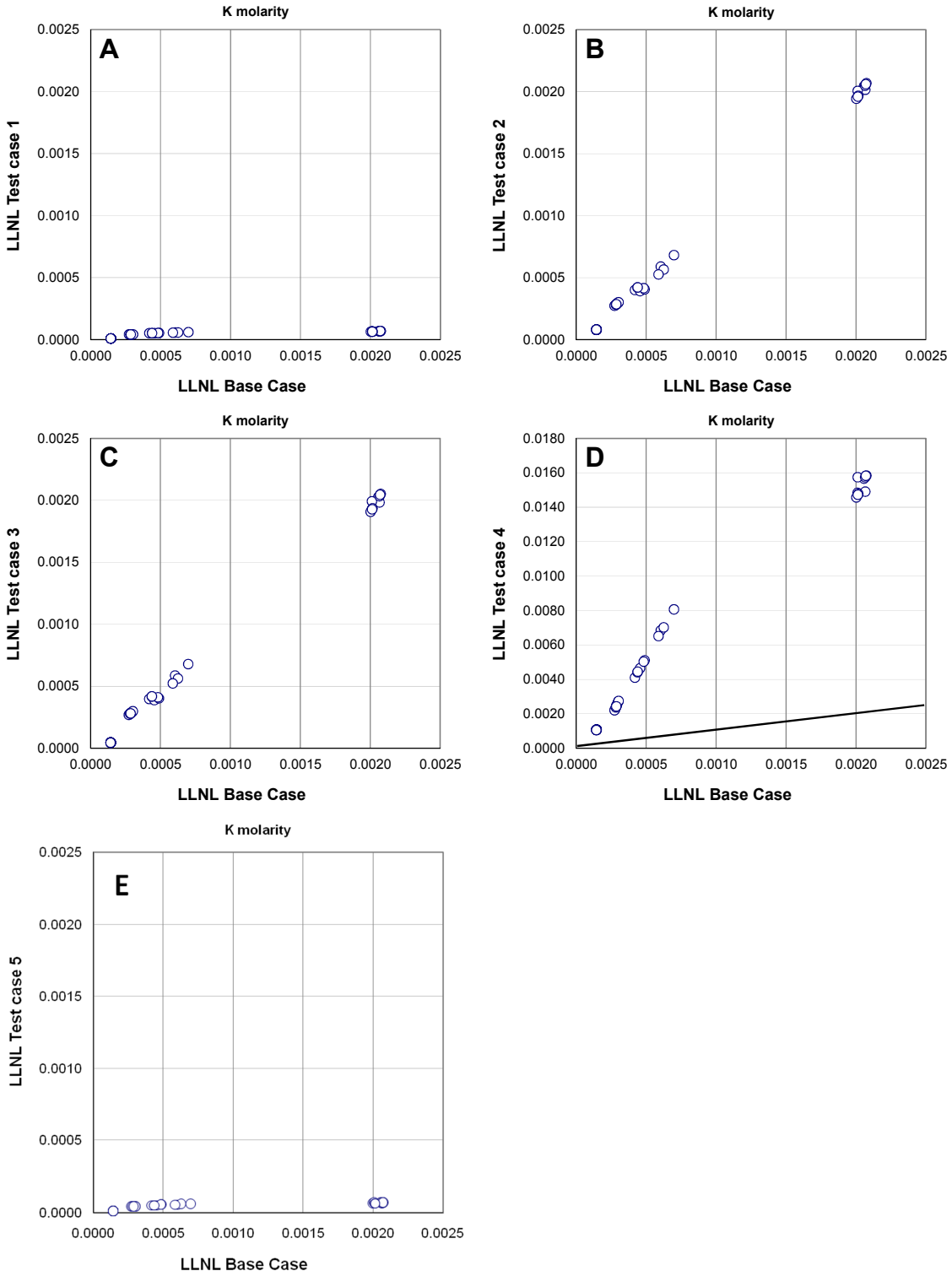

Figure 2-4. *Comparison between the obtained potassium concentrations (in mol/L) in the simulations carried out for the Test Cases 1 to 5 (panels A to E, respectively; see conditions in Table 2-2) and in the simulations done for the Base Case (without aluminosilicate reactions) in the earlier SR-Site calculations performed by Salas et al.(2010). The black line in panel D represents the 1:1 ratio between results of the Test Case 4 and the Base Case.*

Finally, in the Test Case 4 (including illite and a Ca-montmorillonite in the equilibrium set; Table *2-2*), much higher concentrations of dissolved potassium are obtained as compared with the Base Case (Figure 2-4D). In Test Case 4, dissolution of illite and precipitation of montmorillonite promotes exceedingly high potassium concentrations (also affecting the calculated pH values; Figure 2-6D) "never seen" in crystalline systems evolving through pure water-rock interaction processes during long periods of time (see Figure 2-7B), or through mixing processes as, for example, at Forsmark, Laxemar or Olkiluoto (Gimeno et al. 2009, and references therein).

In Laxemar and Olkiluoto the maximum measured concentrations of dissolved potassium (below 0.0008 mol/L) are associated with the deepest and more saline groundwaters whereas, in Forsmark, the highest values (around 0.0018 mol/L) are related to the groundwaters with higher Littorina signature (Gimeno et al. 2009). Note that except in one case, the results obtained for all the waters examined in the Test Case 4 are higher than the aforementioned 0.0018 mol/L (Figure 2-4D).

Therefore, the combination of some specific aluminosilicates in the equilibrium set can provide unrealistic results for potassium[1].

Despite the variations obtained for the concentrations of the other cations with respect to those in the Base Case, their influence in the ***cation safety function indicator*** ($\Sigma q[M^{q+}]$) is minimal in all examined Test Cases as displayed in Figure 2-5; the participation of aluminosilicate minerals seems to have very little effect in the dilute and in the saline waters included in the representative set.

An additional result from the calculations is the fact that, in some cases, the imposed equilibria lead to a ***pH variation*** of up to two pH units in some of the Test Cases (Figure 2-6). In the Base Case, pH values are controlled by calcite dissolution-precipitation reactions after mixing and in the Test Cases variations are caused by the additional effects of aluminosilicate dissolution and precipitation reactions on the pH values.

[1]Potassium is usually a reactive element and a solubility control by sericite or illitic clays or cation exchange processes have been proposed as mechanisms controlling the maxima concentrations of this element (Salas et al. 2010). However, to reproduce the contents of this element by modelling reaction processes is a complicated task even in argillaceous systems with site-specific data, for example using clay solubilities or selectivity coefficients (Pearson et al. 2011). Molinero et al. (2009), trying to reproduce the present hydrochemistry of the groundwaters at Laxemar (from the palaeohydrological history of the site), found that a conservative transport model (mixing) fits better the field measurements of potassium than a reactive transport model including reactions with aluminosilicates and cation exchange processes. This would agree with the existence of a control of potassium by mixing, at least in some of the mixing episodes through the history of the sites (Gimeno et al. 2008).

Overall, calcite and aluminosilicate dissolution tend to increase the pH whereas precipitation tends to decrease it. The calculated pH values would depend on the net effect of the involved mineral mass transfers (dissolved or precipitated). For instance, the latter seems to be the more influential on pH in Test Case 4 (Figure 2-6D), in which calcite and montmorillonite precipitation dominate over the simultaneous dissolution of illite, leading to a decrease in the pH values. But, in any case, the change in the calculated pH values promoted by aluminosilicate reactions (always between 6.5 and 9; Figure 2-6) would not be significant with respect to the criterion (pH<11) for the corresponding safety function indicator R1e in SR-Site (SKB 2011).

Additional test cases and overall conclusions

Quite similar results (almost indistinguishable) are obtained for different smectite, montmorillonite and chlorite-type phases, even though: a) in some cases the variations in the equilibrium constants (thermodynamic data) vary several orders of magnitude for different varieties within the same group; or b) in others, unrealistically high values have been obtained for some cation (see above). Extremely coincident results are also obtained using both data bases, LLNL and THERMODDEM (not shown).

The results obtained in this evaluation confirm in general those obtained already in the framework of SR-Can, where a different thermodynamic database was used (Auqué et al. 2006). Apparently, the effects of adding weathering reactions would not drastically modify the simulations results as far as the safety function indicators are concerned. Therefore, the conclusions presented in Salas et al. (2010) for the hydrochemical evolution at Forsmark remain unchanged.

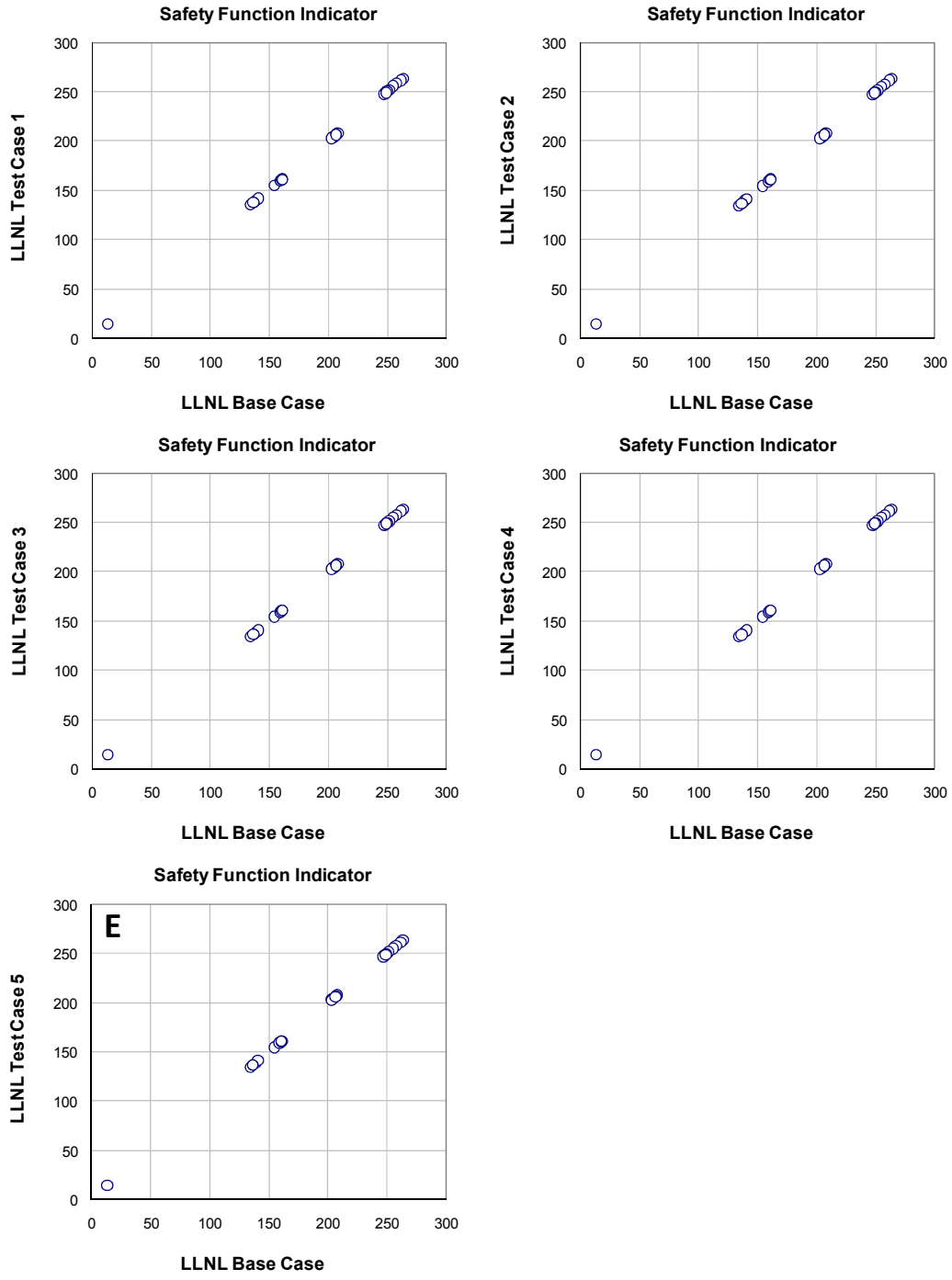

Figure 2-5. *Comparison between the obtained cation safety function indicator values (Σq[Mq+] in mM) in the simulations carried out for the Test Cases 1 to 5 (panels A to E, respectively; see conditions in Table 2-2) and in the simulations done for the Base Case (without aluminosilicate reactions) in the earlier SR-Site calculations performed by Salas et al. (2010).*

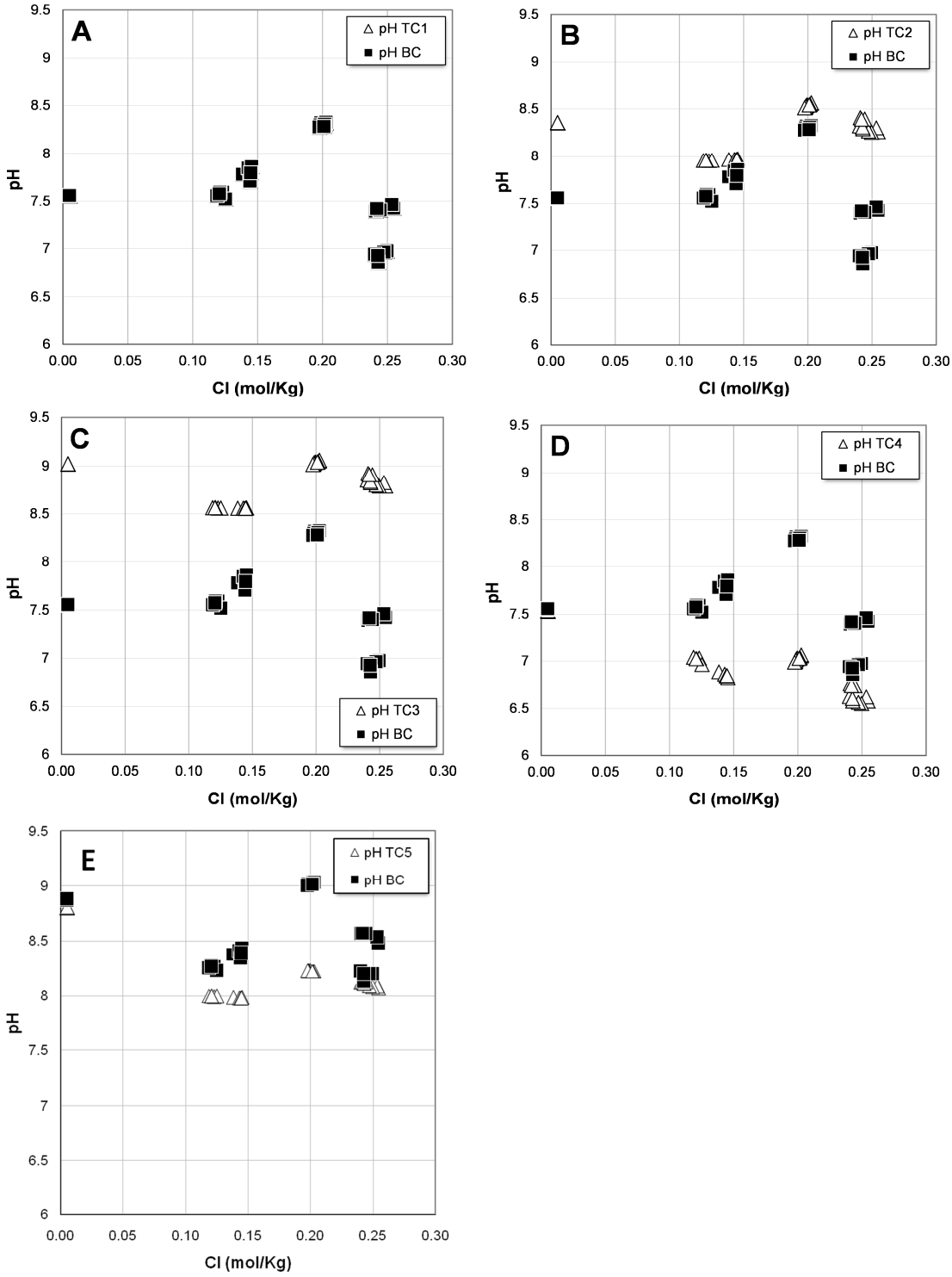

Figure 2-6. *Comparison between the obtained pH values in the simulations carried out for the Test Cases 1 to 5 (panels A to E, respectively; see conditions in Table 2-2) and in the simulations done for the Base Case (without aluminosilicate reactions) in the earlier SR-Site calculations performed by Salas et al. (2010).*

2.3 Evidence from some selected sites

Experimental evidence for the exclusive effects of water-rock interactions (calcite dissolution/precipitation aluminosilicate weathering and ion-exchange reactions) may be found in granitic sites where local hydraulic conditions (*e.g.* high topography) may result in the presence of groundwaters of meteoric origin at large depths, and where saline waters, either ancient or relatively modern (*e.g.* of marine origin), for any reason are not present at the site. Some information on this type of sites was presented in (Auqué et al. 2006, Appendix B) for SR-Can and an additional review of groundwaters from some crystalline systems having predominantly dilute (*i.e.* fresh) waters has been performed here. Data from the following sites will be evaluated here:

- Kivetty: site in Finland with residence times up to 15,000 years; no postglacial sea water intrusion (Anttila et al. 1999a, Pitkänen et al. 1996, 1998).
- Romuvaara: site in Finland with residence times up to (10,000 ± 2000) years; no evidence of postglacial sea water intrusion (Anttila et al. 1999b, Pitkänen et al. 1996).
- Klipperås: site in Sweden; no evidence intrusion of glacial meltwaters or of postglacial sea water (Milnes 2002, Smellie et al. 1987).
- Fjällveden: site in Sweden; no signs of postglacial sea water intrusion (Ahlbom et al. 1991, Bath 2005, Milnes 2002, Smellie et al. 1985).
- Palmottu: natural analogue study site in Finland (U-Th mineralisation); groundwater residence times up to 11,000 years; no postglacial sea water intrusion (Ahonen et al. 2004, Blomqvist et al. 2000, Pitkänen et al. 2002).
- Mizunami: underground research laboratory in Japan; the low-salinity groundwaters have residence times larger than 50,000 years (Iwatsuki et al. 2005, Yamamoto et al. 2013).
- Kamaishi: U-mine in Japan; groundwater residence times up to 3,000 years (Sasamoto et al. 2012).

All the reviewed sites represent stable hydrogeological systems where fracture zones have been exposed to dilute recharge during considerably long periods of time. Water-rock interaction processes (without mixing with saline waters) control the hydrochemical evolution of the groundwaters. Groundwater residence times in these systems range from 3000 BP to > 50,000 BP as indicated above (also indicated in Figure 2-7F). Despite these long residence times, all the examined groundwaters show a dilute character (Cl < 210 mg/L; most of them, < 100 mg/L). The bedrock (both metamorphic and plutonic rocks) and fracture fillings in contact with the groundwaters in these systems are variable in detail but, overall, they show common characters to those found in the Forsmark (or Laxemar) sites.

Figure 2-7 shows the major compositional characteristics of the reviewed groundwaters. In most cases the statistical calculations have been done over sets of waters from shallow and recent derived meteoric groundwaters to the deepest (up to 1000 m at Kivetty and Klipperås), oldest and more evolved groundwaters representing a "complete" hydrochemical evolutive trend. All the systems show low contents in the major components, in the same range or, frequently lower, than those found in the fresh shallow groundwaters from Forsmark or Laxemar:

- Dissolved sulphate concentrations are lower than 20 mg/L and, most frequently < 10 mg/L.
- Chloride contents are more variable but they are always below 211 mg/L. The highest concentrations are found at Mizunami site (Japan) where groundwaters reach the longest residence time (>50,000 years BP). However, the existence of mixing processes between meteoric derived and more saline groundwaters can not be discarded in this system. If the Mizunami groundwaters are not considered, the chloride concentrations are, usually, below 100 mg/L.
- Alkalinity values are always below 150 mg/L (Figure 2-7C).

- The main cations, sodium and calcium, also show low contents. Sodium concentrations are below 70 mg/L (except, again, in the Mizunami groundwaters; Figure 2-7A) whereas dissolved calcium is below 40 mg/L in all cases (Figure 2-7D).
- Dissolved potassium and magnesium show even lower concentrations, below 4 mg/L and 10 mg/L, respectively (Figure 2-7 B and E).
- Finally, pH values range from 7.2 to 9.2 in all examined systems (except at Kamaishi site in Japan, where pH values as high as 10.5 were measured).

Most of the reviewed systems show a clear evolutionary trend from shallow Ca–HCO_3 type groundwater in the upper part of the bedrock to a Na–HCO_3 type in the more mature groundwaters at increasing depth, a typical trend for granitic groundwater systems dominated by water-rock interaction. In the best studied systems (e.g. Kivetty and Romuvaara in Finland), the data show that after an initial enrichment in the cation concentrations at the shallowest levels there is an overall decrease in calcium, magnesium and potassium and a parallel increase in sodium with depth and residence time of the groundwaters.

The main non-redox processes involved in the evolution of these groundwaters (identified and/or modelled) are dissolution/precipitation of calcite, silicate weathering reactions (including precipitation of secondary silicates during hydrolysis reactions, acting as a sink for the observed depletion in magnesium and potassium) and cation exchange processes. The hydrochemical evolution of the reviewed systems reflects the net effects of complex water-rock interaction processes active during long residence times (Figure 2-7; 3000 to more than 50,000 years) and therefore they represent suitable systems where the effects of aluminosilicate reactions must be more important.

Available results from geochemical modelling for some of these sites (e.g. Kivetty and Romuvaara) indicate that the mass transfers associated to dissolution-precipitation of the aluminosilicates, calcite and cation exchange processes differ in their relative importance depending on the system (though always with low absolute values).

In summary, the data from these sites shows that water-rock interactions alone are unable to increase the salinity high enough to fulfil the safety function indicator criterion R1c ($\sum q[M^{q+}] > 4$ mM charge equiv.), despite the fact that the groundwaters have residence times high enough to expect a clear influence of weathering reactions in their hydrochemical evolution. All other safety function indicators criteria considered in SR-Site (SKB 2011) are satisfied, and all these waters are reducing, as described in the corresponding references.

The data also shows the large importance of the geological and hydrogeological conditions as well as the palaeohistory of a granitic site in determining the salinity of its groundwaters, and that water-rock interactions alone have only minor effects on the concentrations of “major” (*i.e.* soluble) groundwater components.

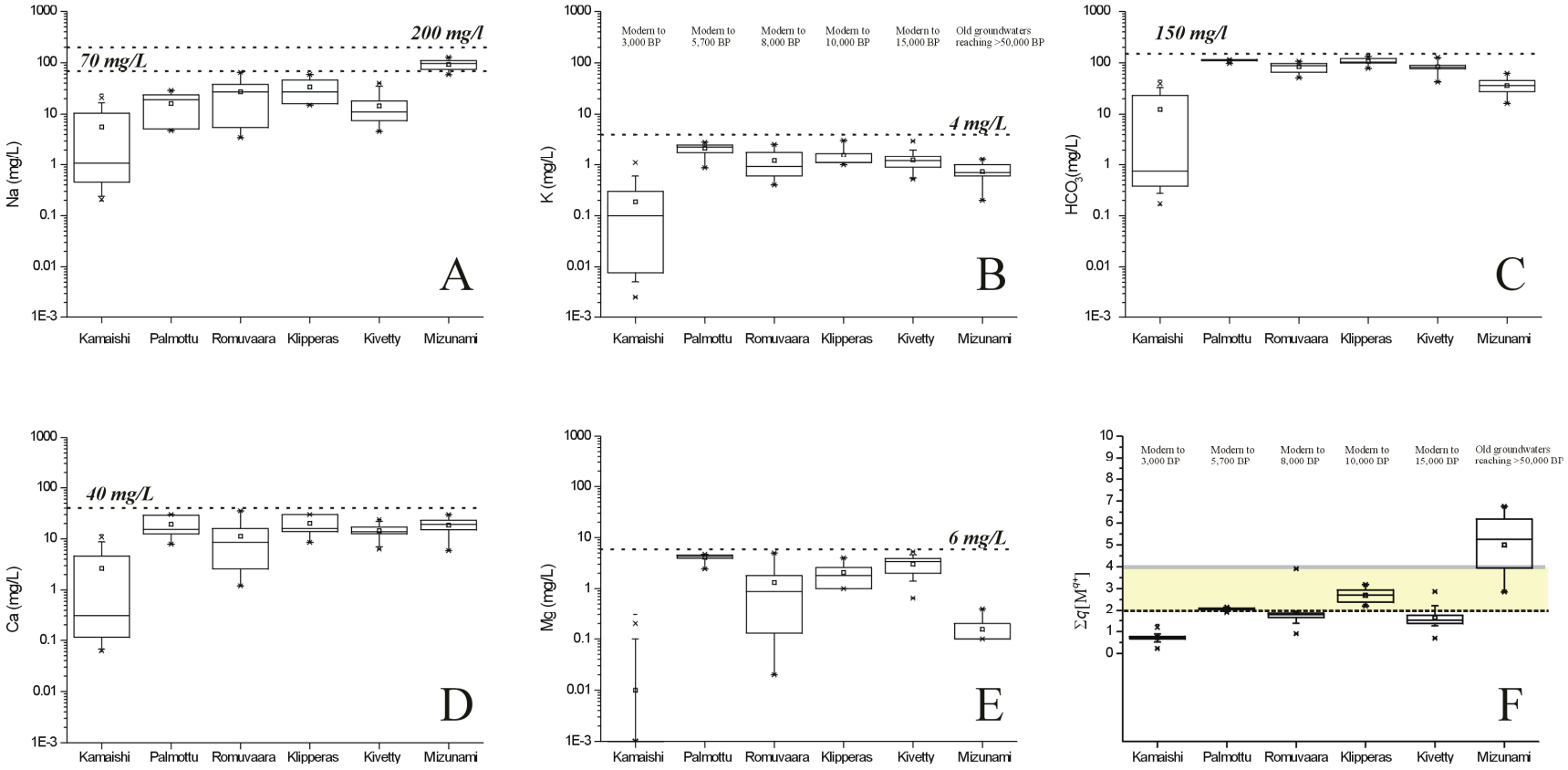

Figure 2-7. *Box-and-whisker plots showing the statistical distribution of the values for dissolved sodium (A), potassium (B), alkalinity (C), calcium (D) and magnesium (E) concentrations (in mg/L) and the calculated value of the cation safety function indicator (F; Σq[Mq+] in mmol/L) in the groundwaters of the reviewed crystalline systems (Kamaishi and Mizunami in Japan; Palmottu, Romuvaara and Kivetty in Finland; Klipperås in Sweden). The statistical measures plotted are the median (horizontal line inside the grey or red box), the 25th and 75th percentiles (bottom and top of the box), the mean (square), the 5th and 95th percentiles ("whiskers"), the 1st and 99th percentile (crosses) and the maximum and the minimum values (horizontal bars).*

3 Cation-exchange

Cation exchange reactions are kinetically fast and can exert an important control on the concentrations of the major cations in groundwaters (Appelo and Postma 2005, Drever 1988). These reactions may be especially active during mixing processes as the difference in the salinity of the mixed groundwaters exerts a major control on the intensity and selectivity of the exchangers for the different cations (Appelo and Postma 2005). This is the reason why the effects of cation exchange processes on the evolution of the groundwaters were taken into account since the first steps in the SKB's site characterization programs and their importance in the hydrochemical evolution of Laxemar and Forsmark was carefully evaluated by (Gimeno et al. 2008, 2009).

However, within the SR-Site, despite their potential importance, cation exchange processes were not included in the final Forsmark report (Salas et al. 2010) for different reasons:

- the calculation methodology needed to properly include these processes in the mixing and reaction simulations was under development and testing at that time;
- the available data on the cation exchange capacities (CEC) values for fracture filling minerals, the composition of the exchange sites and site-specific selectivity coefficients for the exchange reactions (all basic parameters to include cation exchange processes in the simulations) are unavailable or very scarce and uncertain (Byegård et al. 2008, Selnert et al. 2008, 2009); and
- a modification of the thermodynamic database selected for the SR-Site simulations would have been required to include cation exchange processes.

Some partial sensitivity analysis on the influence of cation exchange processes was presented by Gimeno et al. (2010) for the hydrogeochemical evolution of the Laxemar site. Comparative results were presented for year 10,000 AD during the evolution of the temperate period (Appendix 3 in Gimeno et al. 2010). From these results it was concluded that the incorporation of cation exchange processes would not change the overall picture presented about the hydrochemical evolution for the temperate period in Laxemar. However, it was also found that, under some circumstances, the quantitative effect of these processes on some chemical characteristics of the groundwaters (e.g. total concentrations of some elements, pH, *etc*) could be considerable. These aspects were commented in Section 9.5 of Salas et al. (2010) and in Section 6.1 of Gimeno et al. (2010) which dealt with the associated uncertainties in the calculations.

Recently some studies have been initiated with the aim of obtaining CEC values, selectivity coefficients, *etc*, for the fracture fillings from Forsmark, Laxemar and Olkiluoto. Some of these parameters are also of importance for the radionuclide transport and retardation models for these sites (Byegård et al. 2008, Selnert et al. 2009). However, the data are not available yet.

In order to explore the potential effects of cation exchange processes on groundwater modelling, and on the evaluated safety function indicator criterion R1c used in SR-Site ($\sum q[M^{q+}] > 4$ mM charge equiv.), simulations are performed here both of generic character and specific for the Forsmark site using the same method developed by Gimeno et al. (2010) for the Laxemar site. The distribution of clay minerals in the fracture fillings at Forsmark, as the main mineral phases involved in cation exchange processes, is reviewed in the next section.

3.1 Distribution of clay minerals in the fracture fillings at Forsmark

Chlorite (together with calcite) is one of the most abundant minerals identified in the fracture fillings in Forsmark at all examined depths (reaching near 1,000 m; Sandström et al. 2008), see Figure 3-1. Other clay minerals, at lower amounts, have been frequently identified in the Forsmark fracture fillings: corrensite (chlorite/smectite or chlorite/vermiculite mixed layer clay) is the most frequent one followed by illite and other mixed layer clays (*e.g.* illite/smectite; Sandström et al. 2008).

Clay minerals, as the most important phases related with cation exchange processes, show a wide range of CEC values depending on mineral structure, structural substitutions and the specific surface of the mineral accessible to water (Appelo and Postma 2005) and, usually, "pure" (unmixed) chlorite phases have some of the lowest CEC values for clays. However, smectites and vermiculites, and depending on the degree of mixing, the mixed layer clays with these minerals, show the highest CEC values (*e.g.* Appelo and Postma 2005, Drever 1988, White 2013).

These "high-CEC" clay minerals are not evenly distributed in the fractures and, for example, there are differences between the fracture domains differentiated at Forsmark: this type of clay minerals occurs most abundantly in open fractures from the FFM02 domain (Sandström et al. 2008). They are also found more abundantly in fractures in the upper part of the bedrock (in the upper 200 m; Figure 3-1) and less frequently at larger depths (Sandström et al. 2008). Statistical distributions both on total amounts and visible coverage have been reported in Löfgren and Sidborn (2010).

From these data it seems that a certain cation exchange capacity (probably low but it remains to be determined) is widely distributed in the fractures of the bedrock. But the distribution of clay minerals with "nominal" high CEC values in the fracture fillings appears to be highly heterogeneous and, thus, also their possible effects on cation exchange processes. However, in the modelling performed by Gimeno et al. (2010) for Laxemar, and in the calculations presented below for Forsmark, a uniform distribution of ion-exchangers (with equal CEC values) is assumed over the whole studied rock volume (and therefore, in the repository volume). Thus, the effects of cation exchange reactions are assumed to be equally active and important in the whole rock volume.

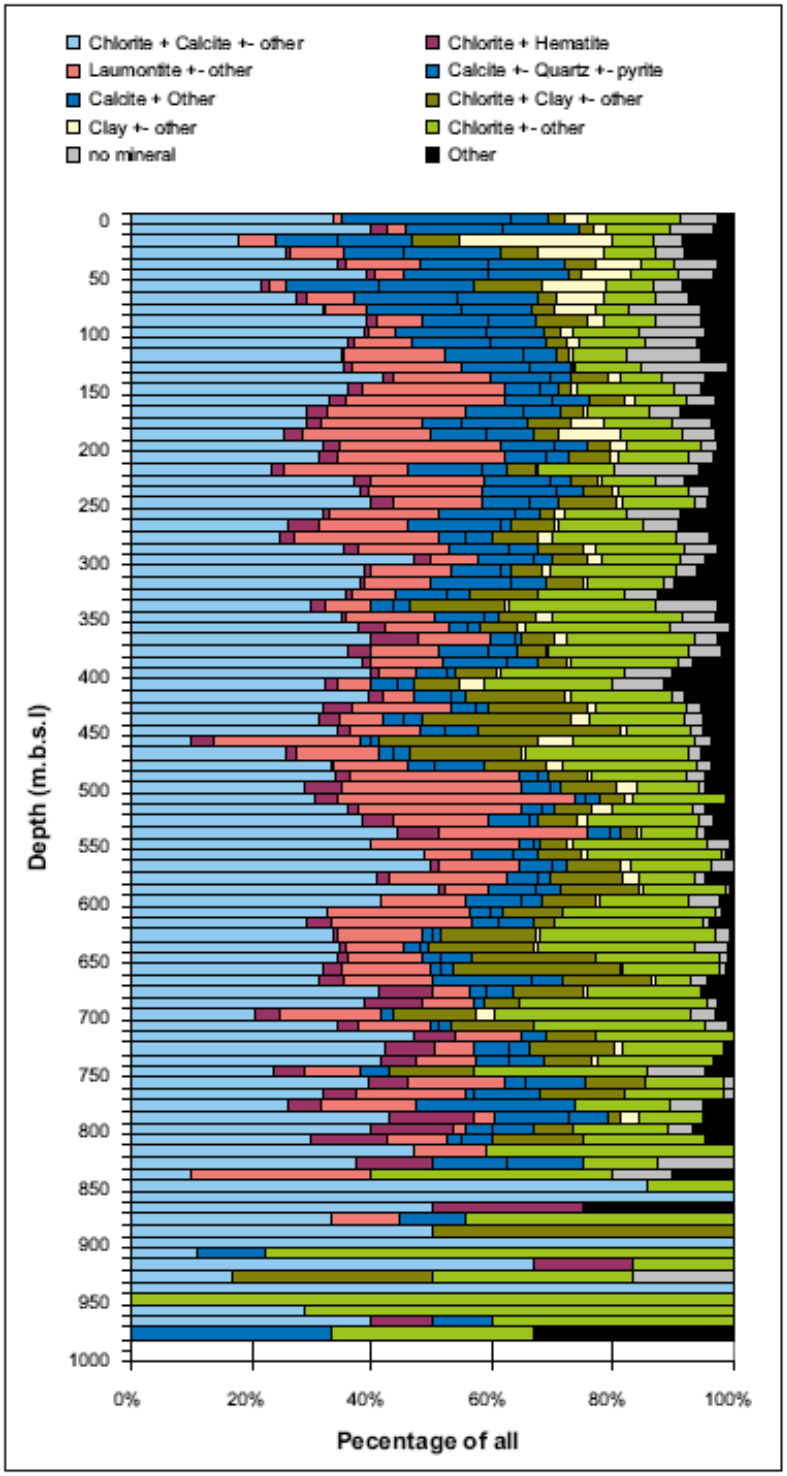

Figure 3-1. *Fracture mineralogy in all open fractures (both in deformation zones and fracture domains) given as percentage of all open fractures at Forsmark. The fracture minerals have been divided into 10 different sets. Corrensite, illite and mixed layer smectite/illite are included as "clay" in the figure. From* Sandström et al. (2008).

3.2 Generic mixing and reaction simulations

The simulated future hydrochemical evolution of the repository zone at Forsmark mainly corresponds to an overall "dilution" originating from the influx of meteoric waters or by the ingress of glacial melt-waters during future glacial periods. "Salinization" scenarios, associated to the possible infiltration of marine waters for short periods of time after a glaciation or related to the upconing of deep saline waters under an advancing or retreating warm-based ice sheet were also identified and evaluated in SR-Site (Salas et al. 2010).

To verify the relative effects of mixing and reaction processes on the safety function indicator R1c ($\sum q[M^{q+}] > 4$ mM charge equiv.) generic simulations, related with the dilution scenario in the temperate period, have been performed here with PHREEQC vers. 2.18 (Parkhurst and Appelo 1999) and the WATEQ4F database (Ball and Nordstrom 1991). Heterogeneous reactions have included both calcite dissolution/precipitation and multi-component cation exchange processes.

3.2.1 Simulation methodology

Mixing calculations (with or without superimposed reactions) have been performed between selected groundwaters sampled at repository depth in Forsmark and an inflowing dilute groundwater of meteoric origin. Complete mixing paths are simulated between these two end-members, from 100 % of the "old", pre-existing groundwaters (OG, described below) to 100 % of dilute groundwater (Altered Meteoric end-member, AM, as used in SR-Site).

Most sampled groundwaters at repository level in the Forsmark candidate area are brackish (Cl between 4,500 and 5,800 mg/L) and have an important Littorina signature (high dissolved magnesium and sulphate). However, there are also some indications of more saline groundwaters (with chloride concentrations around 14,000 mg/L) in KFM07A at the same depth (Gimeno et al. 2008, Laaksoharju et al. 2008). Therefore, a brackish groundwater with important Littorina signature (sample # 8017 from KFM03A at 441 m depth; Table *3-1*) and the only saline non-marine sample available at the repository level (sample #8818 from KFM07A at 379 m depth; Table *3-1*) were selected for the simulations. The selected dilute groundwater corresponds to the equilibrated Altered Meteoric end-member (Table *3-1*) used in the SR-Site calculations for the Forsmark site (see Table 4-2 in Salas et al. 2010).

Table 3-1. Main compositional features of the selected groundwaters (in mg/L) from the repository depth at Forsmark (samples #8017 and #8818 as presented in Gimeno et al. (2008) used in the simulations. The Altered Meteoric end-member composition (Salas et al. 2010) **is also shown.**

	Sample #8017 (KFM03A)	Sample #8818 (KFM07A)	Altered Meteoric end member
Depth (m)	441	379	
Temp	10.7	15.0	15.0
pH	7.29	7.47	7.31
Alk.	91.8	12.4	398.2
Cl	5430	13600	181.2
SO_4^{2-}	472	130	85.1
Na	2070	2840	274.3
K	26.8	15.3	5.6
Ca	985	5150	18.8
Mg	202	34.5	7.5
Sr	1.1	61.1	0.038
SI calcite	0.11	0.0	-0.50

Calcite dissolution/precipitation and cation exchange processes have been superimposed to mixing in the calculations. To properly include cation exchange reactions in the simulations it would be necessary to know the cation exchange capacity (CEC) of the clay minerals in the fracture fillings and the initial composition of the cation-exchange sites. Although the CEC values for the fracture fillings and the initial composition of the exchange sites remains unknown, several indirect CEC estimates are available, mainly deduced from cation exchange modelling in Äspö and Laxemar; see Gimeno et al. (2008, 2009) for a review. The exchange site compositions can be theoretically calculated.

In the following cation exchange calculations a value of 0.5 mol/L for the CEC has been selected according to the literature review performed in Gimeno et al. (2008, 2009). The composition of the exchangers (Table *3-2*) has been calculated with PHREEQC by assuming equilibrium between a generic exchanger and the selected groundwaters at repository depth. The Gaines-Thomas convention (Gaines and Thomas 1953) has been used together with the selectivity coefficients proposed by (Appelo and Postma 1993, 2005), both included in the WATEQ4F database (Ball and Nordstrom 1991) distributed with PHREEQC. Although a generic exchanger (one-site model exchanger) has been considered, the calculated compositions (Table *3-2*) are in the ranges defined, for example, in Viani and Bruton (1995, 1996a, 1996b) for specific minerals (e.g. smectites, illites) in equilibrium with different groundwaters at Äspö and using more complex (multi-site) exchange models. The selectivity coefficients included in the database are usually averages of experimental values obtained for different conditions and environments and, therefore, they are not site-specific values. However, they have provided a good approximation in the modelling of cation exchange processes in different natural systems (e.g. Appelo and Postma 1993, 2005), and even in the site characterisation modelling performed in argillaceous materials (*e.g.* Pearson et al. 2011).

Table 3-2. Calculated exchanger compositions (expressed as equivalent fraction) in equilibrium with the selected brackish/saline groundwaters at the repository depth in Forsmark. Exchanger composition in equilibrium with the Altered Meteoric end-member is also shown for comparison.

	Sample #8017 (KFM03A)	Sample #8818 (KFM07A)	Altered meteoric end-member
CaX_2	0.610	0.812	0.56
MgX_2	0.14	0.006	0.23
NaX	0.24	0.174	0.19
KX	0.009	0.0025	0.011
SrX_2	0.0004	0.0056	0.007

During the mixing + reaction simulations, the initial conditions are defined by the equilibrium between the groundwater existing at repository depth (the brackish marine or the saline non-marine samples in Table *3-1*) and the exchanger in the fracture fillings (Table *3-2*). Under this situation a dilute groundwater (the Altered Meteoric end-member; Table *3-1*) progressively mixes with the already present brackish/saline groundwater, breaking the equilibrium state. Progressive dilution changes the groundwater composition and the exchanger reacts by cation exchange with these new water compositions. Calcite re-equilibrium may also be allowed.

Overall, four type of simulations have been performed with each of the selected groundwaters:

a) pure mixing processes (conservative mixing) between the selected groundwaters;
b) mixing + calcite equilibrium;
c) mixing + multi-component cation-exchange; and
d) mixing + calcite equilibrium + multi-component cation-exchange.

3.2.2 Results from the generic simulations

Figure 3-2 and Figure 3-3 summarize the results of the mixing and reaction simulations with samples #8017 (brackish, Littorina rich groundwater) and #8818 (non-marine saline groundwater), respectively.

The evolution of the total concentration of the dissolved elements (e.g. Ca, Mg, Na, K etc.) during conservative mixing ("only mixing" in Figure 3-2 and Figure 3-3) defines the typical linear trend between the concentrations of the end-members.

Trends for the cation safety function indicator ($\Sigma q[M^{q+}]$) during conservative mixing or mixing + reaction simulations are superimposed and they are mutually indistinguishable at the scale of the graphs.

To clearly differentiate the effects of mixing from those of mixing + reaction simulations in the calculated values of $\Sigma q[M^{q+}]$, a normalisation has been performed using the obtained values of $\Sigma q[M^{q+}]$ in the conservative mixing simulations as reference:

$$\Sigma q[M^{q+}]_{normalised} = \Sigma q[M^{q+}]_{mixing+reactions} / \Sigma q[M^{q+}]_{conservative} \quad \text{(eqn.1)}$$

Results of this normalisation are presented in Figure 3-2E and Figure 3-3E. As it can be observed, normalised values for the mixing + exchange calculations are always equal to one (red spheres) whereas some differences (values different than 1) can be appreciated in the results when calcite equilibrium is overimposed (mixing + calcite equilibrium *versus* mixing + exchange + calcite

equilibrium), especially, when the mixing proportion of the dilute end-member is higher than 50 % (Figure 3-2E and Figure 3-3E).

During conservative mixing (blue spheres in the figures), oversaturation with respect to calcite occurs along most of the simulated mixing path (Figure 3-2D and Figure 3-3D) even if the original end-member waters are at near equilibrium or sub-saturated with respect to calcite, a classical result associated with the non linear behaviour of the ion activity product during mixing (Appelo and Postma 2005, Puigdomenech and Nordström 1987, Wigley and Plummer 1976). Therefore, if calcite equilibrium is imposed (mixing + calcite equilibrium simulations, black crosses), calcium concentrations are slightly reduced compared to conservative mixing. Maximum mass transfers associated to calcite precipitation are around 0.8 mmol/L (in the simulations performed with sample # 8818) but their effects on the dissolved calcium trends are almost indistinguishable from the conservative mixing results obtained for this element (Figure 3-2A and Figure 3-3A, compare the blue spheres and the black crosses).

In mixing + exchange calculations (red spheres), calcium (Figure 3-2A and Figure 3-3A) and magnesium (not shown) concentrations are lower than those obtained in conservative mixing (compare the red and the blue spheres), whereas sodium contents (Figure 3-2B and Figure 3-3B) are higher. Potassium concentrations (not shown) during mixing and exchange calculations are also higher than in conservative mixing simulations except during part of the mixing trend computed with the sample # 8818. These results indicate that calcium and magnesium are selectively fixed to the exchanger whereas sodium is released to the solution.

Calcium fixation in the exchanger during mixing + exchange simulations reduces the calcite oversaturation reached during conservative mixing (Figure 3-2D and Figure 3-3D), and the effect of calcite precipitation on the calcium content is negligible compared with the effect of the exchange. Thus, calcium trends during mixing + exchange and during mixing + exchange +calcite equilibrium simulations are superimposed (Figure 3-2D and Figure 3-3D).

In summary, multicomponent cation exchange processes do not directly modify the $\Sigma q[M^{q+}]$ values imposed by mixing, as expected. Still, cation exchange reactions may affect the $\Sigma q[M^{q+}]$ values through their indirect effects on dissolution/precipitation processes (e.g. calcite equilibrium) although only in minor amounts as shown in these generic simulations. This aspect is further explored in the results described in the next section.

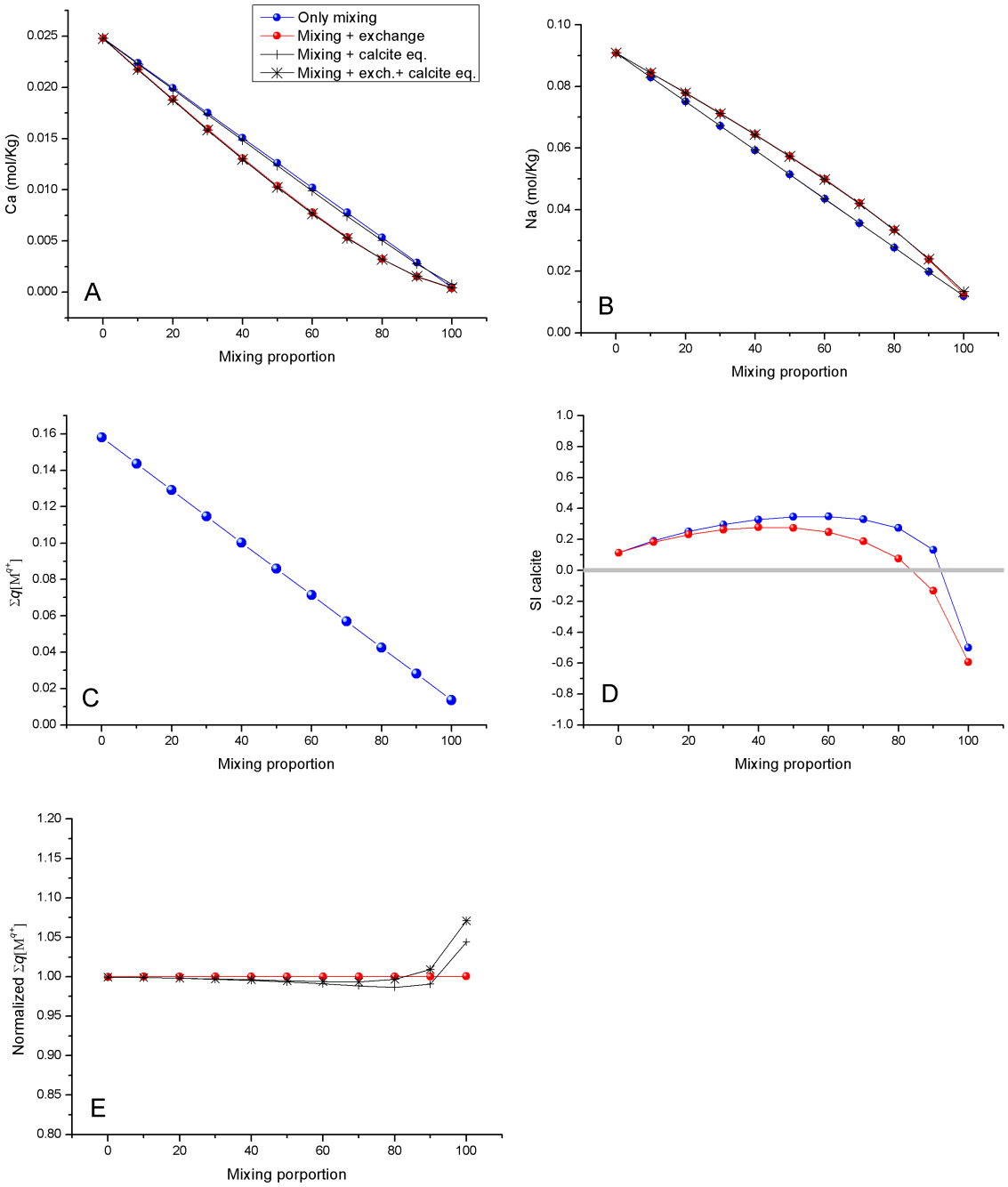

Figure 3-2. *Calcium (A), sodium (B), cation safety function indicator (Σq[Mq+], C), calcite saturation index (SI calcite, D) and normalized Σq[Mq+] (E) values during conservative mixing and mixing + reaction calculations (calcite equilibrium and cation exchange reactions) using sample #8017 as groundwater at the repository depth. The Altered Meteoric end-member was used as the dilute groundwater end-member in all the simulations. Mixing proportions are expressed with respect to the dilute end-member.*

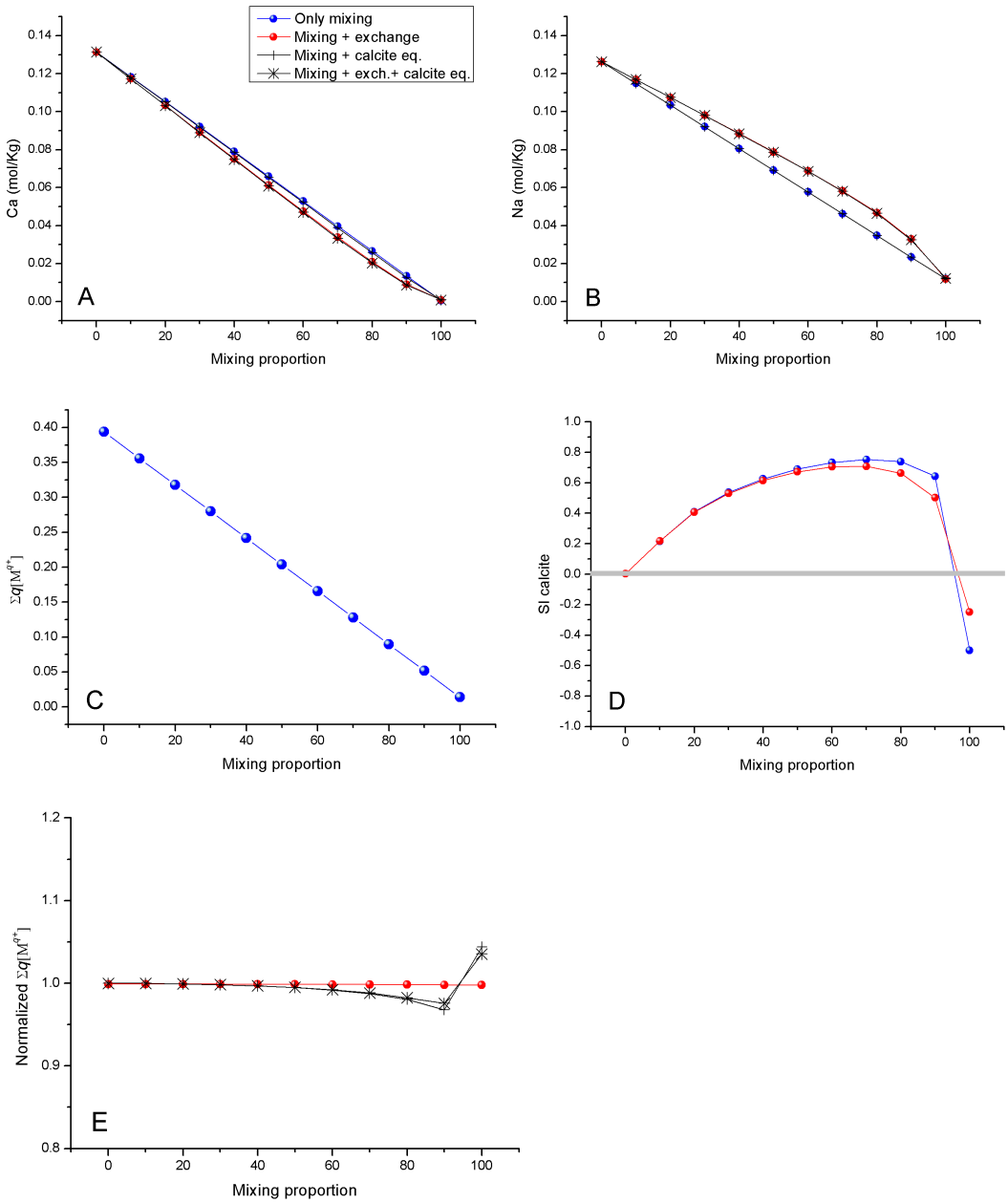

Figure 3-3. *Calcium (A), sodium (B), cation safety function indicator (Σq[Mq+], C), calcite saturation index (SI calcite, D) and normalized Σq[Mq+](E) values during conservative mixing and mixing + reaction calculations (calcite equilibrium and cation exchange reactions) using sample #8818 as groundwater at the repository depth. The Altered Meteoric end-member was used as the dilute groundwater end-member in all the simulations. Mixing proportions are expressed with respect to the dilute end-member.*

3.3 Cation exchange reactions in the hydrochemical evolution during the temperate period at Forsmark

As stated above, except for some periods of saline marine waters intrusion, the simulated future hydrochemical evolution of the repository zone at Forsmark corresponds mainly to an overall "dilution" process driven by the influx of either meteoric waters or by the ingress of glacial melt-water during the future glacial periods (Salas et al. 2010). To explore the potential effects of cation exchange processes on such groundwater evolution, and on the corresponding safety function indicator criterion R1c used in SR-Site ($\sum q[M^{q+}] > 4$ mM charge equiv.), simulations are performed here for the Forsmark site using the same method developed for the Laxemar site (Gimeno et al. 2010).

3.3.1 Methodological approach

The hydrological dataset used in these calculations is the same as that used in Salas et al. (2010) for the evolution of the temperate period in Forsmark. These files include more than two million points in the rock volume of Forsmark, representing the whole regional area of the site down to 2.3 km depth. For the temperate period, the files contain the X-Y-Z coordinates together with the mass fractions of the five reference waters (Deep Saline, Old Meteoric, Glacial, Littorina and Altered Meteoric) for each simulated year: 2000 AD, 3000 AD, 5000 AD and 9000 AD. From these hydrological data files, with the mixing proportions for each data point, different subsets (vertical profiles, N-S, E-W, and a horizontal plane at repository depth) were extracted by Salas et al. (2010) and used to create input files for PHREEQC in order to obtain the detailed chemical composition at each point. In this work, the subsets with the data at repository depth have been used. These subsets correspond to a complete horizontal slice at 440-500 m (with 111,900 points).

The end-member water compositions used to obtain the chemical characteristics of the groundwaters at each point (from the provided mixing proportions) are the same as those used previously in SR-Site (Table 4-2 in Salas et al. 2010). For each point, apart from the mixing, a set of mineral equilibria is also imposed. The selected mineral assemblage is the one used as the Base Case in Salas et al. (2010): calcite + quartz + haematite (with the equilibrium constant proposed by Grenthe et al. 1992)[2]. A more detailed explanation on the overall calculation procedure can be found in Salas et al. (2010).

Implementation of cation exchange processes in the calculations

Cation exchange reactions were already included in the SR-Can simulations as a geochemical variant case (Auqué et al. 2006). Evidently, the cation exchange capacity (CEC) of the clay minerals in the fracture fillings and the initial composition of the exchange sites must be known for such simulations. The model in SR-Can assumed the presence of a unique type of exchanger (*i.e.*, the same CEC and composition for all the grid points in the whole volume and for all the time slices).

Here the presence of a single exchanger at each grid point of the rock volume with the same CEC is also assumed (see section 3.1 above). A value of CEC of 0.5 mol/L has been selected as in section 3.2 from a literature review (Gimeno et al. 2008, 2009).

[2] Haematite-Grenthe with the coupled database has been selected from the different redox variants considered by Salas et al. (2010) as it provides the highest Eh values in the simulations.

Concerning the composition of the exchange sites, the model used in SR-Can (Auqué et al. 2006) was later improved in the Laxemar calculations by Gimeno et al. (2010) by assuming that the composition of the exchanger initially should be in equilibrium at each grid point for the first time slice. Then, the exchanger was transferred to the next time slice, and the new mixed water is equilibrated at each grid point with the exchanger from the previous time slice, modifying, not only the final water composition, but also the composition of the exchanger. In short, the procedure to create the input files for PHREEQC has to take into account the files containing the composition of the cation exchangers and the reaction of waters with them at each grid point. Although changes in the exchanger are transferred from one time slice to the next, changes in water composition are not transferred to the following time slice as they are taken from the hydrogeological model.

Thermodynamic data

The thermodynamic database used for the SR-Site calculations (known as TDB_SKB-2009_Amphos21.dat, SKBdoc id 1261302, vers.3.0) does not have the possibility to deal with cation exchange processes. Therefore, the WATEQ4F database (Ball and Nordstrom 1991) distributed with the code PHREEQC version 2.18 (Parkhurst and Appelo 1999) has been used in the present work. This database includes cation exchange reactions, using the Gaines-Thomas convention (Gaines and Thomas 1953) and the selectivity coefficients reported in Appelo and Postma (1993, 2005).

On the other hand, by comparing the results obtained when using the WATEQ4F database (previously used for SR-Can; Auqué et al. 2006) and those obtained with the SR-Site database, a sensitivity of the results to the thermodynamic data base can be performed. The equilibrium constants for the imposed minerals in equilibrium with the groundwaters (calcite, quartz and haematite-Grenthe) during the simulations performed here are the same than those used in Gimeno et al. (2010) and Salas et al. (2010). Therefore, this sensitivity analysis would mainly be restricted to the thermodynamic data affecting speciation reactions. The same type of sensitivity analysis was carried out by Gimeno et al. (2010) for the results of the hydrochemical evolution at Laxemar.

3.3.2 Results for the hydrochemical evolution at Forsmark including ion-exchange

The comparison of the main compositional characteristics including or excluding cation exchange during the hydrochemical evolution during the temperate period is presented in Figure 3-4 (3000 AD), Figure 3-5 (5000 AD) and Figure 3-6 (9000 AD). Cation exchange reactions affect, directly or indirectly, most of the hydrochemical parameters. As expected ***salinity (TDS)*** is the less influenced parameter (data not shown) and the obtained salinities are in agreement with those presented in Salas et al. (2010).

The incorporation of cation exchange processes affects the calculated ***pH values***, especially in the 5000 AD (Figure 3-5) and 9000 AD (Figure 3-6). In these cases, higher pH values (reaching values near 9 in the 9000 AD period; Figure 3-6) are obtained for a group of groundwaters when cation exchange processes are considered. Therefore, it appears that cation exchange would favour higher pH values in some of the groundwaters at the repository volume during the more “dilute” stages of the temperate period (Figure 3-7). However, the number of groundwaters with pH values higher than 7.9 represent less than 5 % in the repository volume at 9000 AD (Figure 3-7B) and the overall decreasing trend in the pH values during the temperate period obtained in Salas et al. (2010) is still maintained. In any case, the highest pH values obtained in the simulations with cation exchange are still well below pH 11, fulfilling the criterion for the SR-Site safety function indicator R1e.

The calculated ***Eh values*** are also affected by cation exchange processes (as Fe(II) exchange reactions have been allowed; Figure 3-4 to Figure 3-6). However, although the calculated Eh values are slightly more dispersed in the simulations with cation exchange, their statistical distribution, maximum and minimum values and the overall temporal trend along the temperate period do not show significant differences (Figure 3-8 A and B) within the uncertainty of ± 50 mV. The results presented in Salas et al. (2010) indicated a maximum value around −60 mV for the temperate period. Similar values are obtained here, without considering cation exchange (Figure 3-8A), whereas a maximum value around −80 mV is calculated with cation exchange processes (Figure 3-8B). From these results, it appears that the influence of the selected mineral phase to control the Eh values during the hydrochemical evolution is much more important than the effects of the cation exchange processes.

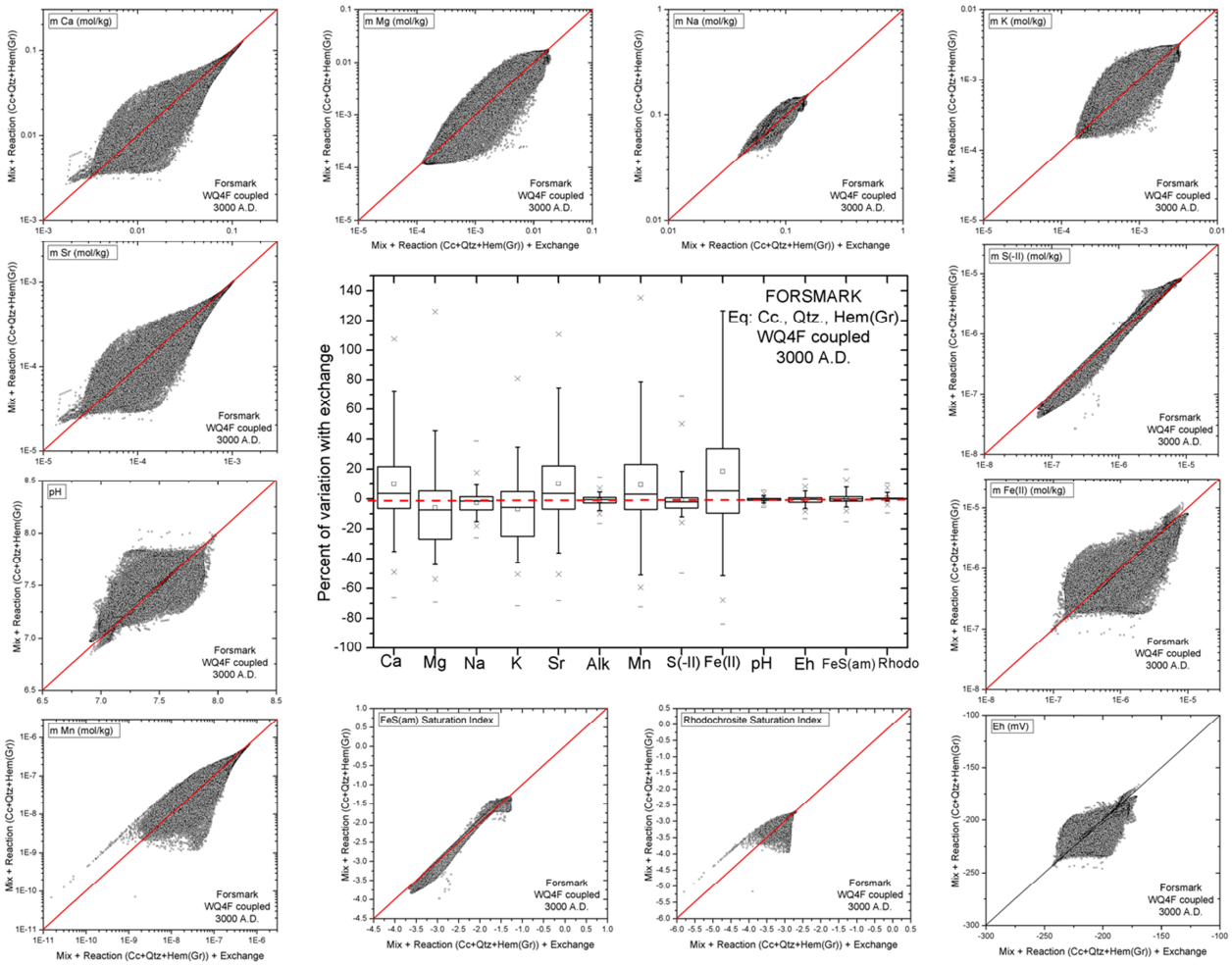

Figure 3-4. *Comparison of the results obtained for Forsmark for the year 3000 AD (Temperate period) in mixing and reaction simulations (considering equilibrium with calcite, quartz, and haematite) with and without cation exchange. X axes indicate the results corresponding to the simulations considering cation exchange processes, and axes Y those obtained not considering these processes. Graph in the middle of the plot show the percent of variation for each parameter when exchange processes are included in the simulations.*

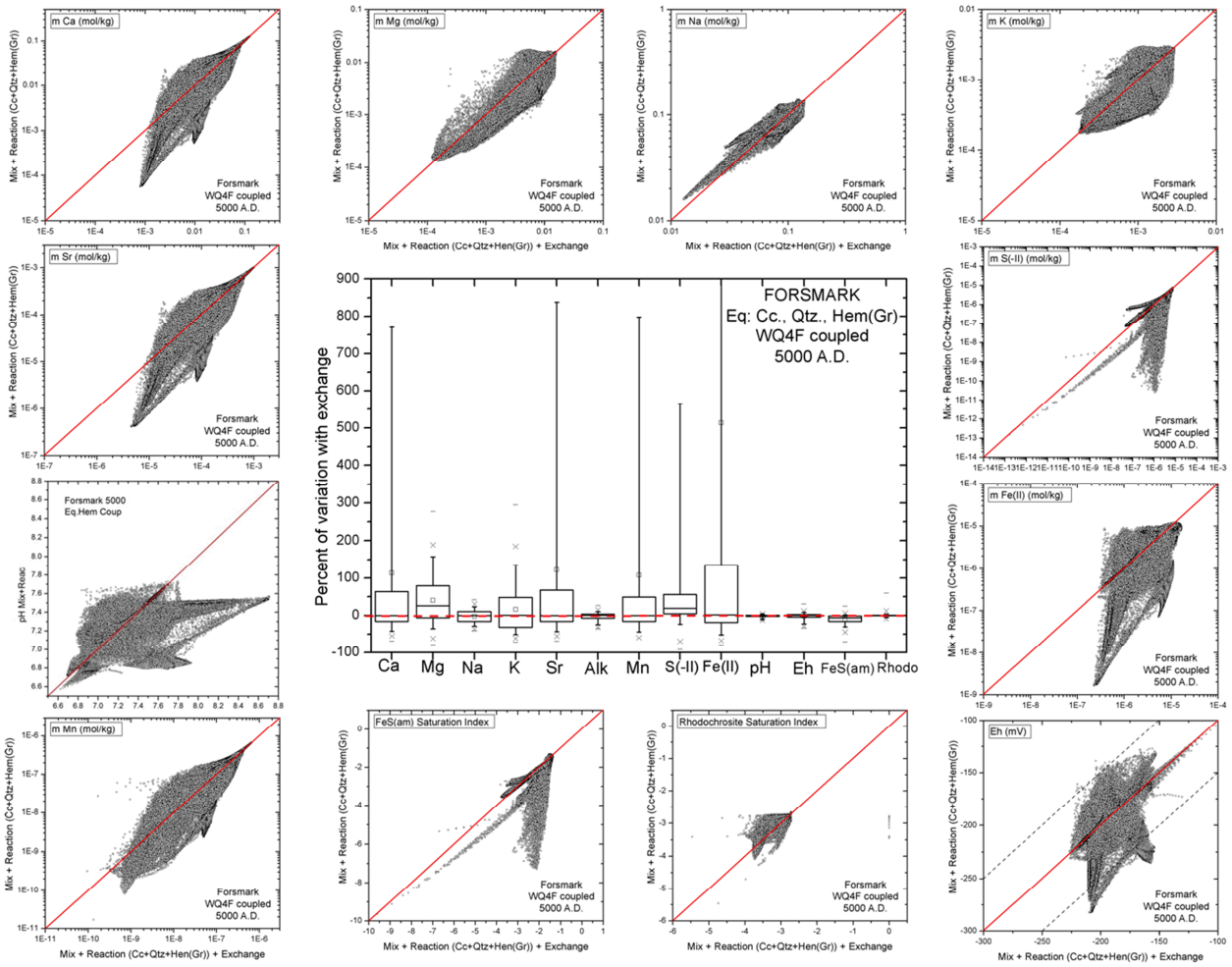

Figure 3-5. *Comparison of the results obtained for Forsmark for the year 5000 AD (Temperate period) in mixing and reaction simulations considering equilibrium with calcite, quartz, and haematite with and without cation exchange. X axes indicate the results corresponding to the simulations considering cation exchange processes, and axes Y those obtained not considering these processes. Graph in the middle of the plot show the percent of variation for each parameter when exchange processes are included in the simulations.*

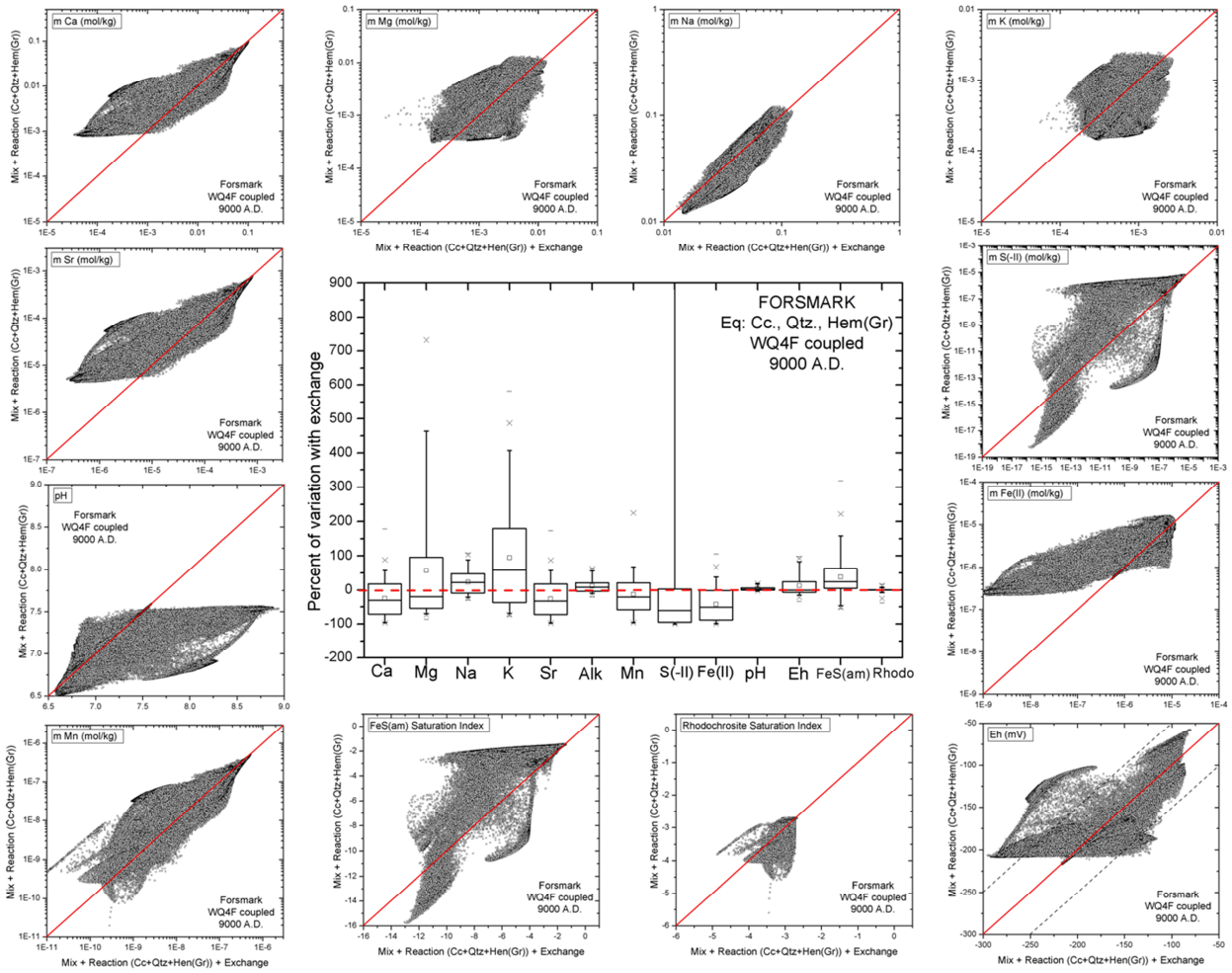

Figure 3-6. *Comparison of the results obtained for Forsmark for the year 9000 AD (Temperate period) in mixing and reaction simulations considering equilibrium with calcite, quartz, and haematite with and without cation exchange. X axes indicate the results corresponding to the simulations considering cation exchange processes, and axes Y those obtained not considering these processes. Graph in the middle of the plot show the percent of variation for each parameter when exchange processes are included in the simulations.*

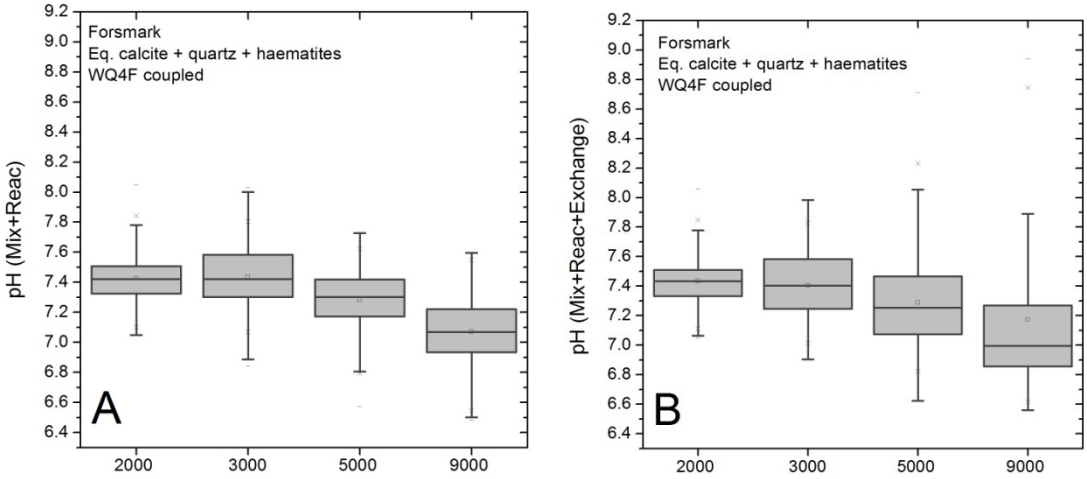

Figure 3-7. *Box-and-whisker plot showing the statistical distribution of the pH (in standard units) calculated over the Temperate period, without (A) and with (B) cation exchange processes, for the groundwaters located within the repository volume at Forsmark.. The statistical measures plotted are the median (horizontal line inside the grey or red box), the 25th and 75th percentiles (bottom and top of the box), the mean (square), the 5th and 95th percentiles ("whiskers"), the 1st and 99th percentile (crosses) and the maximum and the minimum values (horizontal bars).*

Results for ***dissolved Fe(II) and sulphide*** indicate that the maximum concentrations, including the results with and without cation exchange processes, would be lower than $2 \cdot 10^{-5}$ and 10^{-5} mol/L, respectively (Figure 3-4 to Figure 3-6). These values are similar or even lower than those reported in Salas et al. (2010) for the Base Case in the whole temperate period.

The cation concentrations are obviously affected by cation exchange processes with different trends over time depending on the exchanger and groundwater compositions at each point during the simulated stages (Figure 3-4 to Figure 3-6). However, the calculated values for ***the cation safety indicator*** $\Sigma q[M^{q+}]$, with or without cation exchange processes (Sum Cations Mix+Reac+Exch and Sum Cations Mix+Reac, respectively, in Figure 3-9) are the same or indistinguishable at the scale of the plots (Figure 3-9 A,B,C). These results agree with the conclusions reached in section 3.2.

Calcite equilibrium has been allowed in the simulations and this process must affect the calculated $\Sigma q[M^{q+}]$ values, and as stated in section 3.2, cation exchange processes can propagate their effects on $\Sigma q[M^{q+}]$ through mineral dissolution/precipitation processes. To clearly differentiate the indirect effects of cation exchange reactions on $\Sigma q[M^{q+}]$ through calcite equilibrium, the normalisation described above in section 3.2.2, eqn.1, is also used here. These normalised values have been represented *versus* chloride concentrations in Figure 3-9 D,E,F. As it can be seen, the effects of cation exchange processes are apparent in the less saline groundwaters and, especially, in the 5000 and 9000 AD periods when the dilution caused by the calculated influx of upper bedrock-derived meteoric groundwater is more important at repository depth. When the proportion of dilute waters dominates in the mixing processes, higher degrees of disequilibrium with respect to calcite are promoted by the non linear effects of mixing (e.g. Figure 3-9D and Figure 3-10D), and the cation exchange processes affect the amounts of dissolved/precipitated calcite. In any case, the changes indirectly promoted by cation exchange on the $\Sigma q[M^{q+}]$ values are minimal (see the scale of the Y-axes in Figure 3-9 D,E,F). In fact, the statistical distribution of the cation safety function indicator

in the repository volume is virtually identical with or without cation exchange processes (Figure 3-10). As the value of the cation safety function indicator is almost unchanged, the criterion for the safety function indicator is fulfilled.

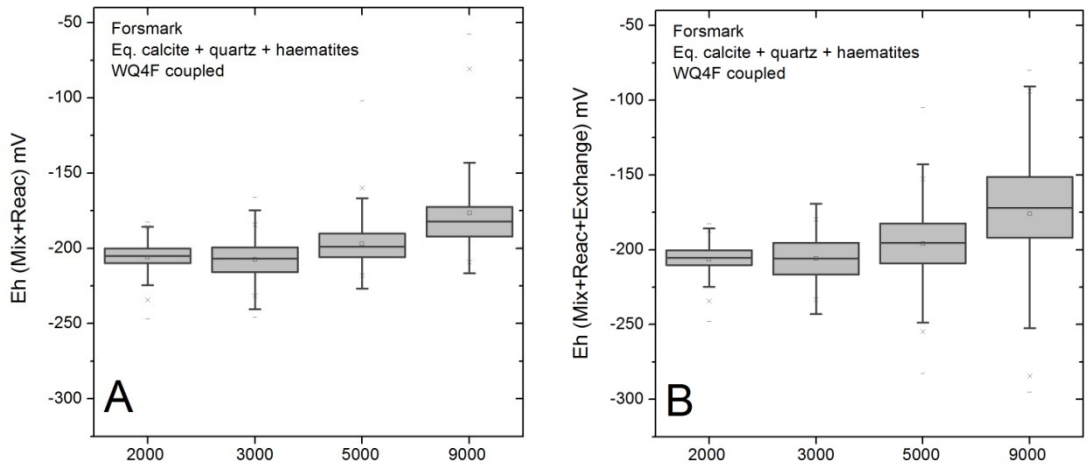

Figure 3-8. *Box-and-whisker plot showing the statistical distribution of the Eh values calculated over the Temperate period, without (A) and with (B) cation exchange processes, for the groundwaters located within the candidate repository volume at Forsmark. The statistical measures plotted are the same as in Figure 3-7.*

Dissolved potassium (safety function indicator R1d in Figure 8.2 from SKB 2011) may be detrimental for the long-term stability of the buffer and backfill (e.g. illitization process). Cation exchange processes affect the dissolved contents of potassium (Figure 3-4 to Figure 3-6) but, as a whole, concentrations are always below $3.5 \cdot 10^{-3}$ mol/L (this value is near to the maximum value found in the used end-members for mixing calculations, the Littorina end-member). In the calculations performed by Salas et al. (2010) the calculated values of dissolved potassium were only controlled by mixing and maximum values of potassium concentrations were also below 0.004 mol/L at any time. Thus, the incorporation of cation exchange processes would not modify this estimation.

Overall, and as evidenced in the performed simulations, cation exchange processes could influence the relative contents of the main cations or the pH values during the hydrochemical evolution of the groundwaters at Forsmark. These effects are more important when the proportion of dilute, meteoric waters dominates (as it was stated in previous studies about the effects of mixing and cation exchange at Äspö (Viani and Bruton 1995, 1996a, 1996b).

However, and as far as we are interested in the evaluation of geochemical safety function indicators, the effects of the cation exchange processes have negligible effects on the conclusions reached by Salas et al. (2010). This is especially true for the cation safety function indicator, $\Sigma q[M^{q+}]$, a conservative parameter with respect cation exchange processes.

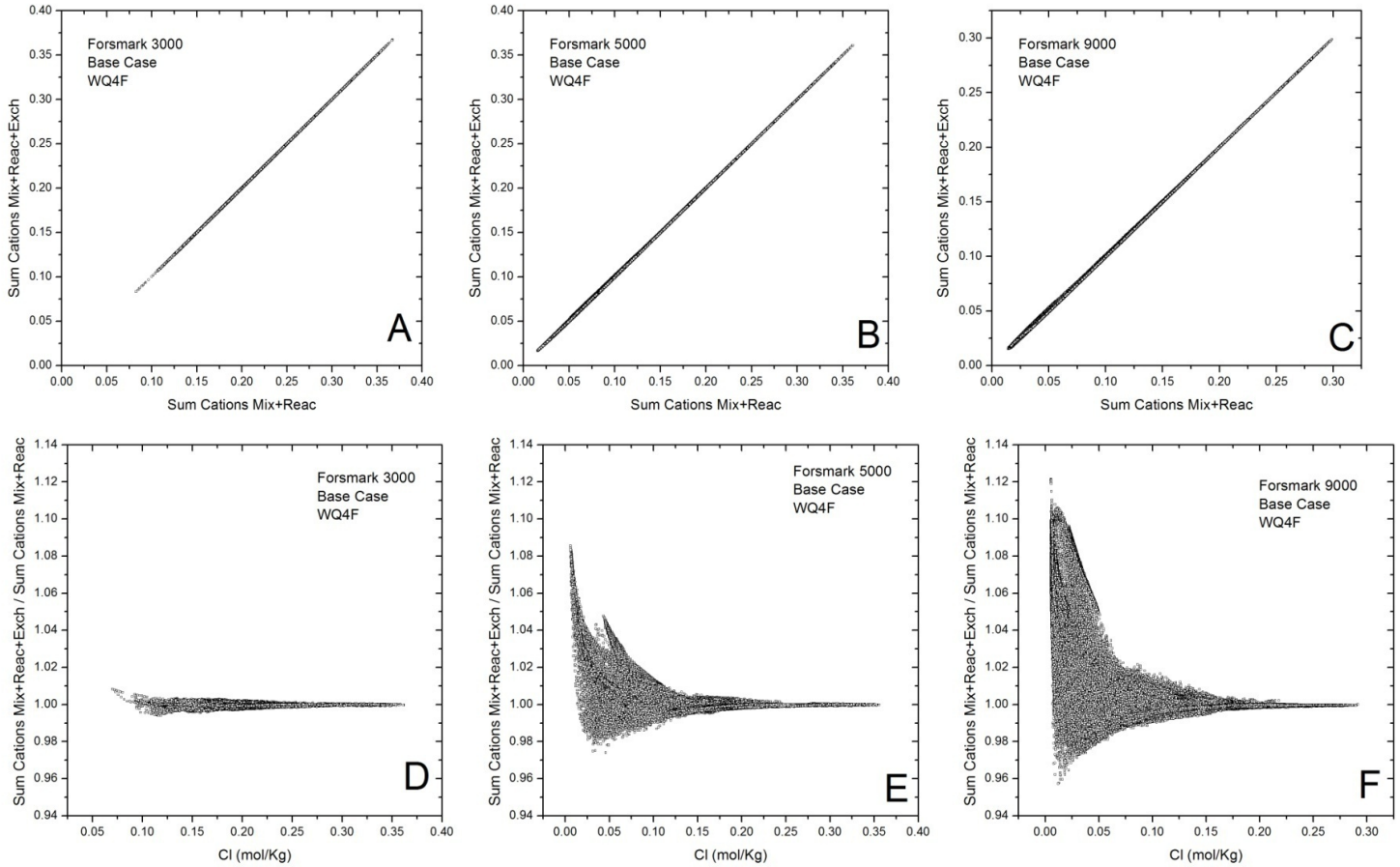

Figure 3-9. *Above: values of the cation safety function indicator (Sum. Cations, Σq[Mq+]) excluding cation exchange (Mix+Reac, X axes) vs values incluiding cation exchange processes (Mix+React+Exchange; Y axes) for the different stages of the Temperate period, 3,000 (A), 5,000 (B) and 9,000 A.D. (C). Below: normalised Σq[Mq+] values vs chloride contents for the same evolutionary stages of the Temperate period, 3,000 (D), 5,000 (E) and 9,000 A.D. (F) at Forsmark.*

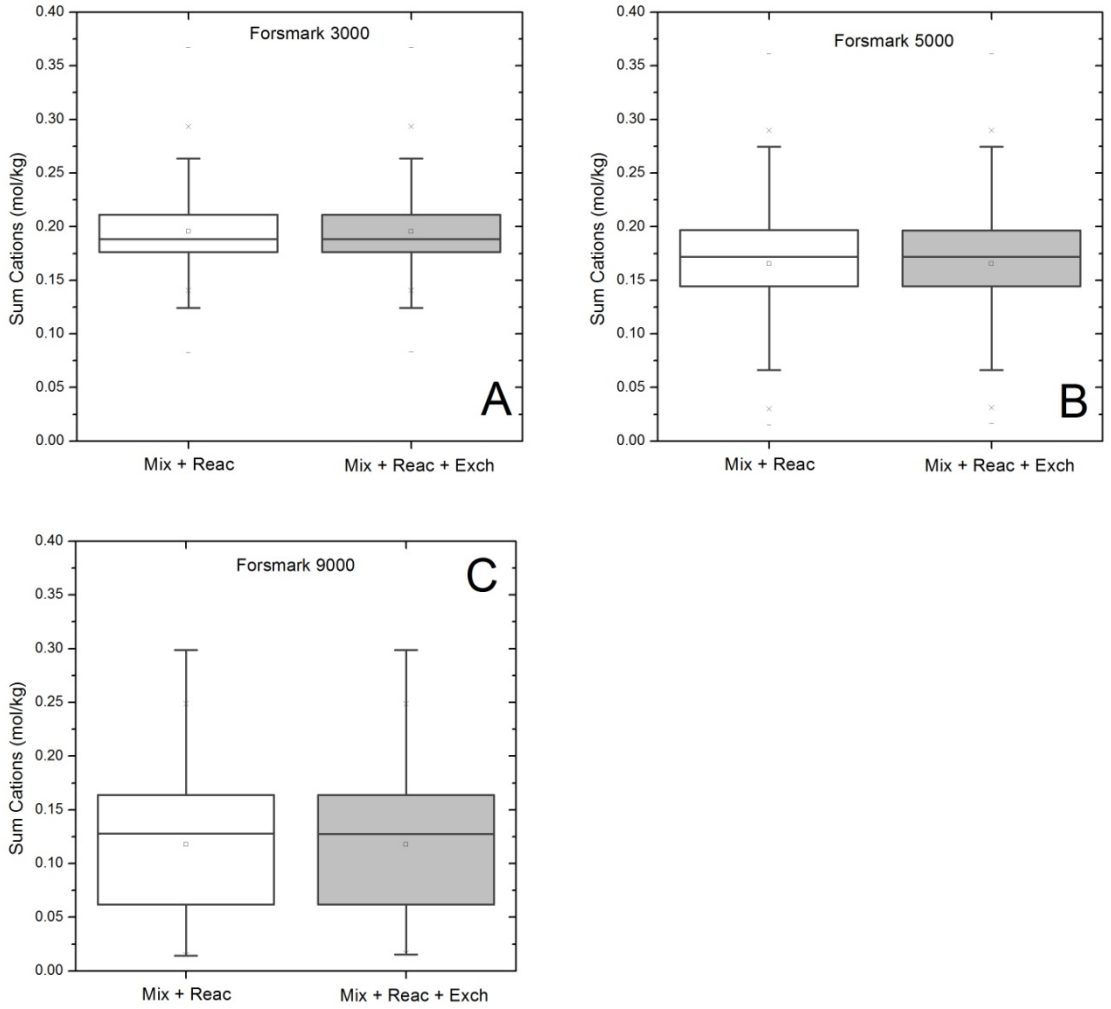

Figure 3-10. *Box-and-whisker plots showing the statistical distribution in the repository volume of the cation safety function indicator (Sum. Cations, Σq[Mq+]) excluding (Mix+React) and including (Mix+React+Exchange) cation exchange processes for the different stages of the Temperate period, 3000 (A), 5000 (B) and 9000 A.D. (C). The statistical measures plotted are the same as in Figure 3-7.*

4 Conclusions

4.1 Aluminosilicate weathering

Mixing and reaction simulations with a few selected representative groundwater mixtures among those used in Salas et al. (2010) have been repeated, adding different sets of aluminosilicate minerals at equilibrium, as well as different thermodynamic databases. This approach allows evaluating the effect of the strongest possible influence of aluminosilicate reactions on the target groundwater hydrochemistry. The aluminosilicate minerals considered in the simulations have been selected from those present as fracture fillings in conductive fractures at Forsmark (chlorite, illite, smectites and feldspars). The calculations indicate that the incorporation of aluminosilicate phases (as additional equilibrium conditions) in the mixing and reaction simulations induces changes in the concentrations

of some individual cations and in the pH values as compared with those presented in Salas et al. (2010):

- The effect on the cation safety function indicator ($\Sigma q[M^{q+}]$) is negligible.
- The effects on the pH values or on the dissolved potassium concentrations do not change the conclusions stated in Salas et al. (2010) concerning the safety function indicators (R1e and R1d, respectively).

Though limited, the sensitivity analysis performed with respect to the thermodynamic data for the aluminosilicate phases (by using different thermodynamic databases) also supports these results (not shown in the figures). The conclusion is that the inclusion of aluminosilicate reactions would not change the conclusions obtained in Salas et al. (2010) about the safety function indicators during the hydrochemical evolution at Forsmark.

In order to evaluate the possible effects of aluminosilicate weathering during a prolonged temperate period, a literature review has been performed on suitable crystalline system exposed for meteoric recharge during considerably long periods of time and controlled by water-rock interaction processes, without mixing with saline waters. In all these sites the groundwaters are clearly diluted, even for those with long average residence times for the groundwaters, showing that water-rock reactions alone are not able to increase the salinity high enough to fulfil the safety function indicator criterion R1c ($\sum q[M^{q+}] > 4$ mM charge equiv.).

The data from these low-temperature sites shows therefore the importance of the geological and hydrogeological conditions as well as the palaeohistory of a granitic site in determining the salinity of its groundwaters, and that water-rock interactions alone have only minor effects on the concentrations of "major" (*i.e.* soluble) groundwater components.

4.2 Ion-exchange

The effects of cation exchange processes on the geochemical safety indicators during the hydrochemical evolution of Forsmark have been evaluated. Site-specific data (CEC values and composition of the exchange complex in the exchangers of the fracture fillings, selectivity coefficients for exchange reactions, etc) are still unavailable and, thus, cation exchange reactions have been included using the same approach (and assumptions) as previously used by Gimeno et al. (2010) for the Laxemar site. This methodology assumes a uniform distribution of an ion-exchanger (with a constant CEC value) over the whole studied rock volume (in contrast with the available mineralogical information) and, therefore, the effects of cation exchange reactions are considered equally active and important in the whole modelled volume. This has, most probably, exaggerated the real effect of this process in the simulations. Nevertheless, the results indicate that the incorporation of cation exchange processes affect directly or indirectly most of the hydrochemical parameters to different degrees, but the incorporation of cation exchange does not change the conclusions presented in Salas et al. (2010) for Forsmark or by Gimeno et al. (2010) for Laxemar concerning the geochemical safety function indicators used in SR-Site.

Salinity (TDS) is the less influenced parameter and clearly remains controlled by mixing. Thus, the related safety function indicator (R1b) is not affected by cation exchange processes.

The calculated pH values are affected by cation exchange reactions and they show higher and lower values than those obtained in the simulations without cation exchange, especially in situations where the dilute end-member dominates and, in Forsmark, higher calculated pH values (with differences near one pH unit but below 9) are obtained for some groundwaters during the more "dilute" stages of the temperate period. It may be noted that except in very particular situations (mafic rock dominated

environments or alkaline thermal waters), it is hard to find groundwaters with pH >11 in crystalline systems even in those with extremely large groundwater ages.

The evaluation of the safety function indicators related with redox parameters (R1a and R1d) are not affected by cation exchange processes. The calculated variations in the Eh values are usually smaller than the uncertainties in measurements (± 50 mV) and the maxima contents of dissolved Fe(II) and sulphide do not virtually change. It may be shown that the selected redox controlling processes in the simulations (mineral phase, coupled or un-coupled database) has a deeper influence on these parameters than cation exchange.

Cation exchange processes affect the dissolved contents of potassium but, as a whole, the maximum concentrations (used to discuss the safety function indicator R1d, Figure 8.2 from SKB 2011) remain unchanged.

The modelling results obtained here indicate that the safety function indicator R1c ($\Sigma q[M^{q+}]$) is not directly affected by ion-exchange reactions. The definition of this safety indicator and the stoichiometry, mass and charge balance constraints in exchange reactions imply that the value for $\Sigma q[M^{q+}]$ in the groundwaters is independent of cation exchange processes. This important conclusion is also true if cation exchange processes are modelled kinetically, rather than as equilibrium processes as in this work. Cation exchange processes may however affect $\Sigma q[M^{q+}]$ indirectly through dissolution-precipitation processes affecting the dissolved cations, although the simulations performed here indicate that this type of indirect effects is very weak.

References

Ahlbom K, Andersson J-E, Nordqvist R, Ljunggren C, Tirén S, Voss C, 1991. Fjällveden study site. Scope of activities and main results. SKB TR 91-52, Svensk Kärnbränslehantering AB.

Ahonen L, Kaija J, Paananen M, Hakkarainen V, Ruskeeniemi T, 2004. Palmottu natural analogue: A summary of the studies. Report YST-121, Geological Survey of Finland.

Anttila P, Ahokas H, Front K, Heikkinen E, Hinkkanen H, Johansson E, Paulamäki S, Riekkola R, Saari J, Saksa P, Snellman M, Wikström L, Öhberg A, 1999a. Final disposal of spent nuclear fuel in Finnish bedrock – Kivetty site report. Posiva 99-09, Posiva Oy, Finland.

Anttila P, Ahokas H, Front K, Hinkkanen H, Johansson E, Paulamäki S, Riekkola R, Saari J, Saksa P, Snellman M, Wikström L, Öhberg A, 1999b. Final disposal of spent nuclear fuel in Finnish bedrock – Romuvaara site report. Posiva 99-11, Posiva Oy, Finland.

Appelo C A J, Postma D, 1993. Geochemistry, groundwater and pollution. Rotterdam: Balkema.

Appelo C A J, Postma D, 2005. Geochemistry, groundwater and pollution. 2nd ed. Rotterdam: Balkema.

Aradóttir E S P, Sonnenthal E L, Jónsson H, 2012. Development and evaluation of a thermodynamic dataset for phases of interest in CO_2 mineral sequestration in basaltic rocks. Chemical Geology 304-305, 26–38.

Arcos D, Grandia F, Domènech C, 2006. Geochemical evolution of the near field of a KBS-3 repository. SKB TR-06-16, Svensk Kärnbränslehantering AB.

Auqué L F, Gimeno M J, Gómez J B, Puigdomenech I, Smellie J, Tullborg E-L, 2006. Groundwater chemistry around a repository for spent nuclear fuel over a glacial cycle. Evaluation for SR-Can. SKB TR-06-31, Svensk Kärnbränslehantering AB.

Ball J W, Nordstrom D K, 1991. User's manual for WATEQ4F, with revised thermodynamic data base and test cases for calculating speciation of major, trace, and redox elements in natural waters. Open-File Report 91-183, U.S. Geological Survey, Menlo Park, California.

Bath A, 2005. Geochemical investigations of groundwater stability. SKI Report 2006:12, Swedish Nuclear Power Inspectorate.

Bath A, 2011. Infiltration of dilute groundwaters and resulting groundwater compositions at repository depth. Report 2011:22, Swedish Radiation Safety Authority.

Beaucaire C, Michelot J-L, Savoye S, Cabrera J, 2008. Groundwater characterisation and modelling of water-rock interaction in an argillaceous formation (Tournemire, France). Applied Geochemistry 23, 2182–2197.

Blomqvist R, Ruskeeniemi T, Kaija J, Ahonen L, Paananen M, Smellie J, Grundfelt B, Pedersen K, Bruno J, Pérez del Villar L, Cera E, Rasilainen K, Pitkänen P, Suksi J, Casanova J, Read D, Frape S, 2000. The Palmottu natural analogue project Phase II: Transport of radionuclides in a natural flow system at Palmottu. EUR 19611 EN, Luxembourg: Office for Official Publications of the European Communities.

Bucher K, Zhang L, Stober I, 2009. A hot spring in granite of the Western Tianshan, China. Applied Geochemistry 24, 402–410.

Byegård J, Selnert E, Tullborg E-L, 2008. Bedrock transport properties. Data evaluation and retardation model. Site descriptive modelling, SDM-Site Forsmark. SKB R-08-98, Svensk Kärnbränslehantering AB.

Cama J, Ganor J, Ayora C, Lasaga C A, 2000. Smectite dissolution kinetics at 80°C and pH 8.8. Geochimica et Cosmochimica Acta 64, 2701–2717.

Drake H, Sandström B, Tullborg E-L, 2006. Mineralogy and geochemistry of rocks and fracture fillings from Forsmark and Oskarshamn: Compilation of data for SR-Can. SKB R-06-109, Svensk Kärnbränslehantering AB.

Drever J I, 1988. The geochemistry of natural waters. 2nd ed. Engelwood Cliffs, NJ: Prentice Hall.

Gailhanou H, van Miltenburg J C, Rogez J, Olives J, Amouric M, Gaucher E C, Blanc P, 2007. Thermodynamic properties of anhydrous smectite MX-80, illite IMt-2 and mixed-layer illite-smectite ISCz-1 as determined by calorimetric methods. Part I: Heat capacities, heat contents and entropies. Geochimica et Cosmochimica Acta 71, 5463–5473.

Gailhanou H, Rogez J, van Miltenburg J C, van Genderen A C G, Grenèche J M, Gilles C, Jalabert D, Michau N, Gaucher E C, Blanc P, 2009. Thermodynamic properties of chlorite CCa-2. Heat capacities, heat contents and entropies. Geochimica et Cosmochimica Acta, 73, 4738–4749.

Gailhanou H, Blanc P, Rogez J, Mikaelian G, Kawaji H, Olives J, Amouric M, Denoyel R, Bourrelly S, Montouillout V, Vieillard P, Fialips C I, Michau N, Gaucher E C, 2012. Thermodynamic properties of illite, smectite and beidellite by calorimetric methods: enthalpies of formation, heat capacities, entropies and Gibbs free energies of formation. Geochimica et Cosmochimica Acta, 89, 279–301.

Gaines G L, Thomas H C, 1953. Adsorption studies on clay minerals. II. A formulation of the thermodynamics of exchange adsorption. Journal of Chemical Physics 21, 714–718.

Gaucher E C, Tournassat C, Pearson F J, Blanc P, Crouzet C, Lerouge C, Altmann S, 2009. A robust model for pore-water chemistry of clayrock. Geochimica et Cosmochimica Acta 73, 6470–6487.

Gérard F, Fritz B, Clément A, Crovisier J-L, 1998. General implications of aluminium speciation-dependent kinetic dissolution rate law in water–rock modelling. Chemical Geology 151, 247–258.

Gimeno M J, Auqué L F, Gómez J B, Acero P, 2008. Water–rock interaction modelling and uncertainties of mixing modelling. SDM-Site Forsmark. SKB R-08-86, Svensk Kärnbränslehantering AB.

Gimeno M J, Auqué L F, Gómez J B, Acero P, 2009. Water–rock interaction modelling and uncertainties of mixing modelling. Site descriptive modelling, SDM-Site Laxemar. SKB R-08-110, Svensk Kärnbränslehantering AB.

Gimeno M J, Auqué L F, Gómez J B, Salas J, Molinero J, 2010. Hydrogeochemical evolution of the Laxemar site. SKB R-10-60, Svensk Kärnbränslehantering AB.

Grenthe I, Stumm W, Laaksuharju M, Nilsson A-C, Wikberg P, 1992. Redox potentials and redox reactions in deep groundwater systems. Chemical Geology 98, 131–150.

Grimaud D, Beaucaire C, Michard G, 1990. Modelling of the evolution of ground waters in a granite system at low temperature: the Stripa ground waters, Sweden. Applied Geochemistry 5, 515–525.

Huertas F J, Caballero E, Jiménez de Cisneros C, Huertas F, Linares J, 2001. Kinetics of montmorillonite dissolution in granitic solutions. Applied Geochemistry 16, 397–407.

Iwatsuki T, Furue R, Mie H, Ioka S, Mizuno T, 2005. Hydrochemical baseline condition of groundwater at the Mizunami underground research laboratory (MIU). Applied Geochemistry 20, 2283–2302.

Klein E, De Lucia M, Kempka T, Kühn M, 2013. Evaluation of long-term mineral trapping at the Ketzin pilot site for CO_2 storage: an integrative approach using geochemical modelling and reservoir simulation. International Journal Of Greenhouse Gas Control 19, 720–730.

Köhler S J, Dufaud F, Oelkers E H, 2003. An experimental study of illite dissolution kinetics as a function of pH from 1.4 to 12.4 and temperature from 5 to 50°C. Geochimica et Cosmochimica Acta, 67, 3583–3594.

Laaksoharju M, Smellie J, Tullborg E-L, Gimeno M, Hallbeck L, Molinero J, Waber N, 2008. Bedrock hydrogeochemistry Forsmark. Site descriptive modelling, SDM-Site Forsmark. SKB R-08-47, Svensk Kärnbränslehantering AB.

Lasaga A C, Soler J M, Ganor J, Burch T E, Nagy K L, 1994. Chemical weathering rate laws and global geochemical cycles. Geochimica et Cosmochimica Acta 58, 2361–2386.

Löfgren M, Sidborn M, 2010. Statistical analysis of results from the quantitative mapping of fracture minerals in Forsmark. Site descriptive modelling – complementary studies. SKB R-09-30, Svensk Kärnbränslehantering AB.

Milnes A G, 2002. Swedish deep repository siting programme. Guide to the documentation of 25 years of geoscientific research (1976–2000). SKB TR-02-18, Svensk Kärnbränslehantering AB.

Molinero J, Salas J, Arcos D, Duro L, 2009. Integrated hydrogeological and geochemical modelling of the Laxemar-Simpevarp area during the recent Holocene (las 8,000 years). Contribution to SDM-Site Laxemar. Hydrochemistry background report. In Kalinowski B E (ed). Background complementary hydrogeochemical studies. Site descriptive modelling, SDM-Site Laxemar. SKB R-08-111, Svensk Kärnbränslehantering AB, 47–78.

Parkhurst D L, Appelo C A J, 1999. User's guide to PHREEQC (version 2): a computer program for speciation, batch-reaction, one-dimensional transport, and inverse geochemical calculations. Water-Resources Investigations Report 99-4259, U.S. Geological Survey, Denver, Colorado.

Pearson F J, Tournassat C, Gaucher E C, 2011. Biogeochemical processes in a clay formation *in situ* experiment: Part E – Equilibrium controls on chemistry of pore water from the Opalinus Clay, Mont Terri Underground Research Laboratory, Switzerland. Applied Geochemistry 26, 990–1008.

Pitkänen P, Snellman M, Vuorinen U, 1996. Geochemical modelling study on the age and evolution of the groundwater at the Romuvaara site. Posiva 96-06 , Posiva Oy, Finland.

Pitkänen P, Luukkonen A, Ruotsalainen P, Leino-Forsman H, Vuorinen U, 1998. Geochemical modelling of groundwater evolution and residence time at the Kivetty site. Posiva 98-07, Posiva Oy, Finland.

Pitkänen P, Kaija J, Blomqvist R, Smellie J A T, Frape S K, Laaksuharju M, Negrel P, Casanova J, Karhu J, 2002. Hydrogeochemical interpretation of groundwater at Palmottu. In von Maravic H, Alexander W R (eds). Eighth EC Natural Analogue Working Group Meeting. EUR 19118 EN, European Commission, 155–167.

Puigdomenech I, Nordström K, 1987. Geochemical interpretation of groundwaters from Finnsjön, Sweden. SKB TR 87-15, Svensk Kärnbränslehantering AB.

Salas J, Gimeno M J, Auqué L, Molinero J, Gómez J, Juárez I, 2010. SR-Site – hydrogeochemical evolution of the Forsmark site. SKB TR-10-58, Svensk Kärnbränslehantering AB.

Sandström B, Tullborg E-L, Smellie J, MacKenzie A B, Suksi J, 2008. Fracture mineralogy of the Forsmark site. SDM-Site Forsmark. SKB R-08-102, Svensk Kärnbränslehantering AB.

Sasamoto H, Hama K, Seo T, 2012. Characterization of redox conditions in the excavation disturbed zone of a drift in the Kamaishi mine, Japan. Engineering Geology 151, 100–111.

Selnert E, Byegård J, Widestrand H, 2008. Forsmark site investigation. Laboratory measurements within the site investigation programme for the transport properties of the rock. Final report. SKB P-07-139, Svensk Kärnbränslehantering AB.

Selnert E, Byegård J, Widestrand H, Carlsten S, Döse C, Tullborg E-L, 2009. Bedrock transport properties. Data evaluation and retardation model. Site descriptive modelling, SDM-Site Laxemar. SKB R-08-100, Svensk Kärnbränslehantering AB.

Sena C, Salas J, Arcos D, 2010. Aspects of geochemical evolution of the SKB near field in the frame of SR-Site. SKB TR-10-59, Svensk Kärnbränslehantering AB.

Sidborn M, Sandström B, Tullborg E-L, Salas J, Maia F, Delos A, Molinero J, Hallbeck L, Pedersen K, 2010. SR-Site: Oxygen ingress in the rock at Forsmark during a glacial cycle. SKB TR-10-57, Svensk Kärnbränslehantering AB.

SKB, 2011. Long-term safety for the final repository for spent nuclear fuel at Forsmark. main report of the SR-Site project. SKB TR-11-01, Svensk Kärnbränslehantering AB.

Smellie J, Larsson N-Å, Wikberg P, Carlsson L, 1985. Hydrochemical investigations in crystalline bedrock in relation to existing hydraulic conditions: Experience from the SKB test-sites in Sweden. SKB TR 85-11, Svensk Kärnbränslehantering AB.

Smellie J, Larsson N-Å, Wikberg P, Puigdomenech I, Tullborg E-L, 1987. Hydrochemical investigations in crystalline bedrock in relation to existing hydraulic conditions: Klipperås test-site, Småland, Southern Sweden. SKB TR 87-21, Svensk Kärnbränslehantering AB.

Stumpf A R, Elwood Madden M E, Soreghan G S, Hall B L, Keiser L J, Marra K R, 2012. Glacier meltwater stream chemistry in Wright and Taylor Valleys, Antarctica: significant roles of drift, dust and biological processes in chemical weathering in a polar climate. Chemical Geology 322–323, 79–90.

Tournassat C, Alt-Epping P, Gaucher E C, Gimmi T, Leupin O X, Wersin P, 2011. Biogeochemical processes in a clay formation *in situ* experiment: Part F – Reactive transport modelling. Applied Geochemistry 26, 1009–1022.

Trotignon L, Beaucaire C, Louvat D, Aranyossy J-F, 1999. Equilibrium geochemical modelling of Äspö groundwaters: a sensitivity study of thermodynamic equilibrium constants. Applied Geochemistry 14, 907–916.

Viani B E, Bruton C J, 1995. The role of cation exchange in controlling groundwater chemistry at Äspö, Sweden. Report UCRL-JC-119724, Lawrence Livermore National Laboratory, Livermore, CA.

Viani B E, Bruton C J, 1996a. Effect of cation exchange of major cation chemistry in the large scale redox experiment at Äspö. Report UCRL-JC-118592 Rev.1, Lawerence Livermore National Laboratory, Livermore, CA.

Viani B E, Bruton C J, 1996b. Assessing the role of cation exchange in controlling groundwater chemistry during fliud mixing in fractured granite at Äspö, Sweden. Second Äspö International Geochemistry Workshop, Äspö, Sweden, June 6–7, 1995. Report UCRL-JC-121527, Lawrence Livermore National Laboratory, Livermore, CA.

Vieillard P, 2000. A new method for the prediction of Gibbs free energies of formation of hydrated clay minerals based on the electronevativity scale. Clays And Clay Minerals 48, 459–473.

Vieillard P, 2002. A new method for the prediction of Gibbs free energies of formation of phyllosilicates (10 Å and 14 Å) based on the electronegativity scale. Clays And Clay Minerals 50, 352–363.

Wersin P, Stroes-Gascoyne S, Pearson F J, Tournassat C, Leupin O X, Schwyn B, 2011. Biogeochemical processes in a clay formation *in situ* experiment: Part G – Key interpretations and conclusions. Implications for repository safety. Applied Geochemistry 26, 1023–1034.

White W M, 2013. Geochemistry. Oxford, UK: Wiley-Blackwell.

Wigley T M L, Plummer L N, 1976. Mixing of carbonate waters. Geochimica et Cosmochimica Acta 40, 989–995.

Wilson J, Savage D, Cuadros J, Shibata M, Ragnarsdottir K V, 2006. The effect of iron on montmorillonite stability. (I) Background and thermodynamic considerations. Geochimica et Cosmochimica Acta 70, 306–322.

Yamamoto K, Yoshida H, Akagawa F, Nishimoto S, Metcalfe R, 2013. Redox front penetration in the fractured Toki Granite, central Japan: an analogue for redox reactions and redox buffering in fractured crystalline host rocks for repositories of long-lived radioactive waste. Applied Geochemistry 35, 75–87.

Unpublished documents

Joyce S, Woollard H, Marsic N, Sidborn M, 2013. Future evolution of groundwater composition at Forsmark during an extended temperate period. SKBdoc 1416908 ver 1.0, Svensk Kärnbränslehantering AB.

SKBdoc 1261302, vers. 3.0. Thermodynamic database: SKB-09. Svensk Kärnbränslehantering AB.